NEW YORK UNIVERSITY
COURANT INSTITUTE-LIBRARY

IMM 384
September 1970

Courant Institute of
Mathematical Sciences

Supercritical Flow in an Overfall

A. S. Peters

IMM 384 c.1

Prepared under Contract N00014-67-A-0467-0016
with the Office of Naval Research NR 062-160

Distribution of this document is unlimited.

New York University

NEW YORK UNIVERSITY
COURANT INSTITUTE - LIBRARY

NR 062-160

IMM 384
September 1970

NEW YORK UNIVERSITY
COURANT INSTITUTE-LIBRARY

New York University

Courant Institute of Mathematical Sciences

SUPERCRITICAL FLOW IN AN OVERFALL

A. S. Peters

This report represents results obtained at the Courant Institute of Mathematical Sciences, New York University, with the Office of Naval Research, Contract N00014-67-A-0467-0016.
Reproduction in whole or in part is permitted for any purpose of the United States Government.

Distribution of this document is unlimited.

ABSTRACT

This report presents an analysis of supercritical flow in an overfall whose nappes are subjected to different constant pressures. It contains computations for brink depth and approximate equations for the nappes in the neighborhood of the brink and far downstream.

1. Introduction

The shape of the nappes and the brink depth are characteristics of an overfall which have intrigued several analysts who have used numerical methods and various other approximation procedures to explain the falling flow. The purpose of this paper is to investigate a two-dimensional overfall under the assumptions, not adopted hitherto, that the pressures on the nappes are different but constant and that the upstream flow is supercritical.

If the acceleration due to gravity is g, if the upstream depth is a and if the velocity there is u, then the flow is said to be critical if $\varepsilon = ga/u^2$ is equal to unity. Our analysis is based on the supposition that ε is small so that the upstream velocity ($u \gg \sqrt{ga}$) of the flow is supercritical. Such a flow can prevail in a region of space where g is small compared with a and u. It can obviously also prevail if u is sufficiently large, or if a is so small that the overfall degenerates into a falling sheet.

We show below that the velocity potential of the flow must satisfy a provocative nonlinear integral equation involving the parameter ε. Taking ε to be small we examine the consequences of the assumption that the solution of the integral equation possesses an asymptotic expansion in powers of ε. We find that the second order approximation provides results which are sufficiently accurate if ε is small. Even for the critical case $\varepsilon = 1$ it turns out that our analysis gives a depth $b = (.70)a$ in the neighborhood of the brink when the pressure difference $\overline{p}$ for the nappes is zero.

The brink depth of the overfall is of some importance for metering channel flows and (.71)a is the average of approximate values found from the application of other methods to the case $\overline{p} = 0$. Besides a focus of attention on brink depth, we present second order equations for the shapes of the nappes in the neighborhood of the brink and far downstream. We conclude with brief remarks about the overfall in the form of a thin sheet.

2. Formulation

A two-dimensional waterfall or free overfall is defined by its flow in a plane perpendicular to its linear edge. Figure 2.1 shows such a flow referred to a rectangular coordinate system whose origin is at the brink. The negative part of the x-axis coincides

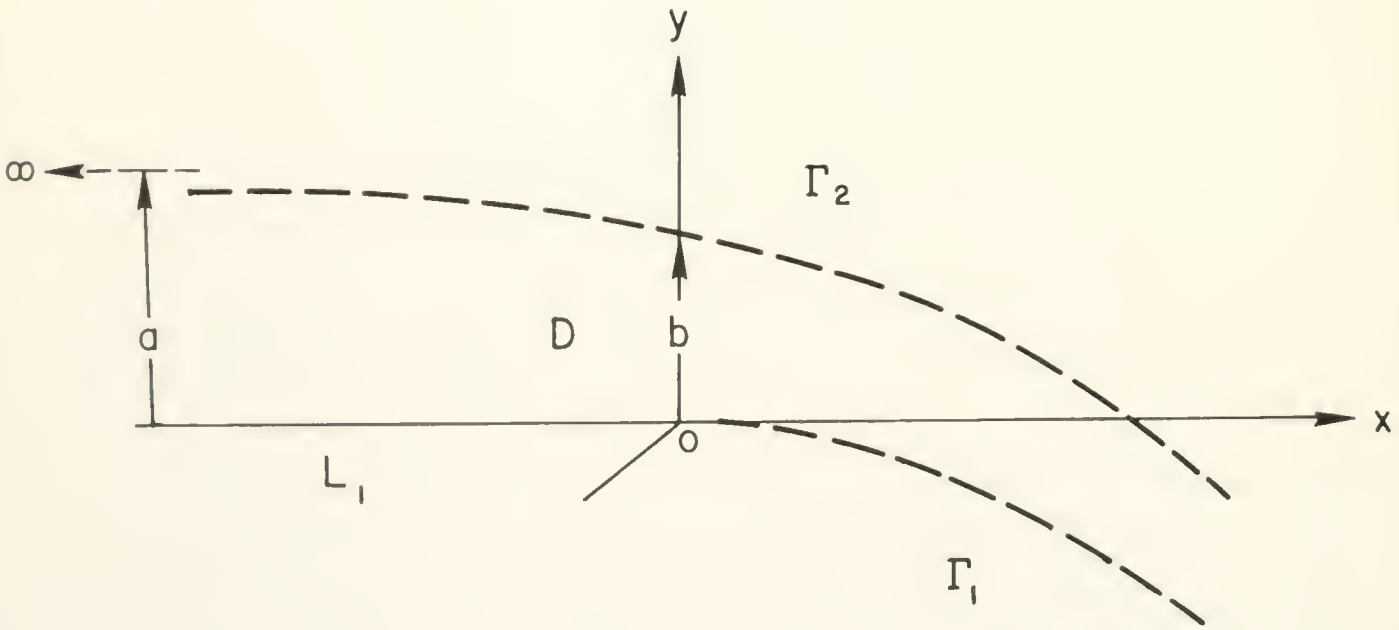

FIG. 2.1

with the sill or bottom L_1 and the y-axis is positive upwards. The domain D of the cross sectional flow is bounded by L_1; and the curves Γ_1 and Γ_2 which define the free surfaces or nappes of the overfall.

The difficult basic problem is to deduce the shapes of Γ_1 and Γ_2 as consequences of the assumptions that gravitational attraction is the only body force acting and that the flow is a steady irrotational one of an inviscid, incompressible fluid whose density δ is constant. If $\underline{v}$ is the velocity vector, conservation of mass requires $\nabla \cdot \underline{v} = 0$ and this with the vorticity condition, $\nabla \times \underline{v} = 0$, insures the existence of a function of the complex variable $z = x + iy$, namely the complex velocity potential,

$$w = \phi(x,y) + i\psi(x,y) = F(z) \tag{2.1}$$

which is analytic for z in D. This function is such that the gradient of its real part gives the velocity vector $\underline{v} = \nabla \operatorname{Re} F(z) = \nabla\phi$; and such that its imaginary part, $\psi = \operatorname{Im} F(z)$, is the stream function for the flow. In other words, the horizontal and vertical velocity components are given respectively by the real and imaginary parts of

$$\overline{F'(z)} = \phi_x - i\psi_x = \psi_y + i\phi_y \ .$$

If $\underline{n}$ is the unit outward normal to the boundary of D and if s denotes arc length along the boundary then the kinematic boundary condition requires that the normal velocity

$$\phi_n = \psi_s$$

must be zero along L_1, Γ_1 and Γ_2. It follows from this, by integration with respect to s, that L_1 plus Γ_1 constitutes a stream line which we can assume is defined by the level curve

$$\psi(x,y) = 0 \ .$$

With this, the upper nappe curve Γ_2 is defined by the level curve

$$\psi(x,y) = h = au$$

where a is the upstream depth of the flow at $x = -\infty$, and u is the velocity there. In addition to the kinematic boundary condition, the energy integral of the momentum equation

$$\delta \frac{d\underline{v}}{dt} = \delta \underline{v} \cdot \nabla \underline{v} = \frac{\delta}{2} \nabla \underline{v} \cdot \underline{v} = -\nabla p - g\delta \nabla y \ ,$$

namely,

$$\phi_x^2 + \phi_y^2 + \frac{2p}{\delta} + 2gy = c \tag{2.2}$$

must be satisfied along Γ_1 and Γ_2. In this equation g denotes the gravitational acceleration and p denotes the pressure in the fluid. Since the flow is supposed to be steady the constant c remains the same no matter where the left hand side is evaluated. Therefore with

$$\phi_x(-\infty, y) = u$$

$$\phi_y(-\infty, y) = 0$$

$$p(-\infty, a) = p_2$$

we have

$$c = u^2 + 2ga + \frac{2p_2}{\delta} \quad . \tag{2.3}$$

Under certain circumstances the pressure p_2 acting on the upper nappe of the overfall is different from the pressure p_1 acting on the lower nappe. For example, wind action on the upper nappe or vapor pressure action under the fall could cause pressure differences. The pressures p_2 and p_1 are not likely to be the same if the overfall is confined between parallel walls perpendicular to the brink and the fall is over a vertical cliff so that the air under the fall is isolated from the rest of the bounding air. For a case like this, intentional pressure differences could be produced. In order to approximately cover these possibilities we suppose that the prescribed pressures p_2 and p_1 are constants such that $p_2 - p_1$ is not large.

Although the domain D is not known at the outset we can work with a fixed domain in the $w = \phi + i\psi$ plane if we introduce the inverse function

$$z = x(\phi, \psi) + iy(\phi, \psi) = G(w) \quad . \tag{2.4}$$

Under the mapping from the z-plane to the w-plane, D is mapped into the strip S defined by

$$0 < \psi = \operatorname{Im} w < h = aw \; ; \quad -\infty < \phi = \operatorname{Re} w < \infty \; ,$$

and we can choose the origin of the w-plane to be the image of the origin of the z-plane. With the origin fixed in this way the images of Σ_1, Γ_1 and Γ_2 are respectively M_1, S_1 and S_2 as shown in Fig. 2.2. Since there are no stagnation points in the overfall,

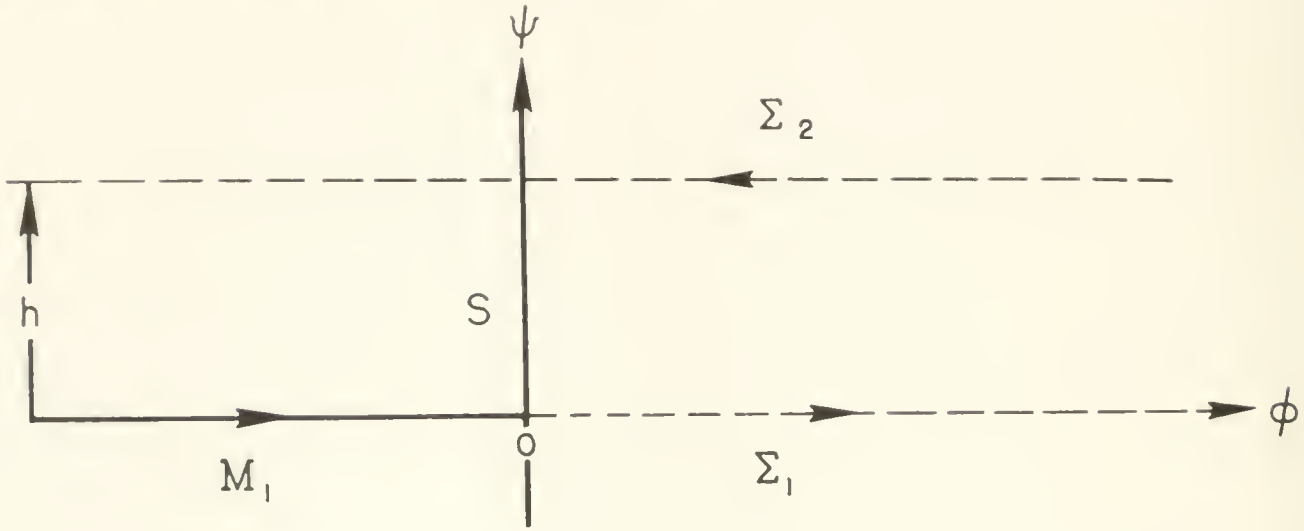

FIG. 2.2

the function G(w) must be analytic in S and we have

$$\frac{dz}{dw} = G'(w) = x_\phi + iy_\phi = -ix_\psi + y_\psi$$

$$= \frac{1}{\frac{dw}{dz}} = \frac{1}{\phi_x + i\psi_x} = \frac{1}{\phi_x - i\phi_y} = \frac{\phi_x + i\phi_y}{\phi_x^2 + \phi_y^2}$$

from which

$$G'(w)\overline{G'(w)} = |G'(w)|^2 = x_\phi^2 + y_\phi^2 = \frac{1}{\phi_x^2 + \phi_y^2}$$

and

$$\phi_x = \frac{\text{Re } G'(x)}{|G'(w)|^2} ; \qquad \phi_y = \frac{\text{Im } G'(w)}{|G'(w)|^2} .$$

These relations with (2.2) and (2.3) show that G(w) must satisfy the following boundary conditions:

$$\text{Im } G'(\phi) = 0 , \qquad \phi < 0 ;$$

$$\frac{1}{|G'(\phi)|^2} + 2g \text{ Im } G(\phi) = u^2 + 2ga + \frac{2(p_2 - p_1)}{\delta} , \qquad \phi > 0 ;$$

$$\frac{1}{|G'(\phi + ih)|^2} + 2g \text{ Im } G(\phi + ih) = u^2 + 2ga , \qquad -\infty < \phi < \infty .$$

We can now map into any domain we think may be helpful for the analysis, whether strictly numerical or not. Instead of the strip S in the w-plane we are going to transform the problem into one for the upper half of the complex ζ-plane into which S is mapped by

$$\zeta = -e^{-\pi w/h} .$$

Under this mapping the images of M_1, Σ_1, and Σ_2 are respectively L_1^*, Γ_1^* and Γ_2^* as shown in Fig. 2.3. The image of the brink 0 in

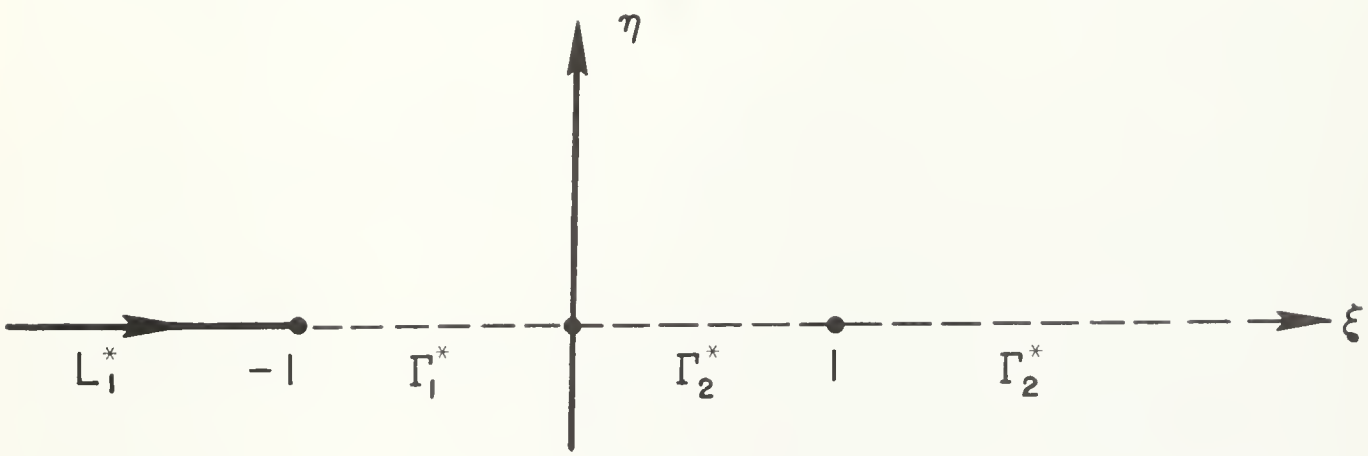

FIG. 2.3

the z-plane is now at $\zeta = -1$ while the source and sink of the overfall become respectively the point at infinity and the origin in the ζ-plane. We also have

$$G(w) = G[\frac{h}{\pi} \ln (-\frac{1}{\zeta})] = \Omega(\zeta)$$

$$G'(w) = -\frac{\pi\zeta}{h}\Omega'(\zeta) \ .$$

The problem now is to find the function $\Omega(\zeta)$ which is analytic for Im $\zeta > 0$ and satisfies the boundary conditions

$$\text{Im}\,\Omega'(\xi) = 0 \ , \qquad \xi < -1 \ ; \tag{2.5}$$

$$\frac{h^2}{\pi^2\xi^2|\Omega'(\xi)|^2} = u^2 + 2ga(1+\bar{p}) - 2g\ \text{Im}\,\Omega(\xi) \ , \qquad -1 < \xi < 0 \ ; \tag{2.6}$$

$$\frac{h^2}{\pi^2\xi^2|\Omega'(\xi)|^2} = u^2 + 2ga - 2g\ \text{Im}\,\Omega(\xi) \ , \qquad 0 < \xi \ ; \tag{2.7}$$

where

$$\bar{p} = \frac{p_2 - p_1}{\delta g a} \ .$$

For the neighborhood of infinity $-\pi\zeta\Omega'(\zeta)$ must behave like

$$-\pi\zeta\Omega'(\zeta) \sim hG'(w)\Big|_{\phi=-\infty} \sim \frac{h(\phi_x + i\phi_y)}{\phi_x^2 + \phi_y^2}\Big|_{x=-\infty}$$

$$\sim \frac{h}{u} = a \ .$$

By integrating the condition $\text{Im}\,\Omega'(\xi) = 0$ we find $\text{Im}\,\Omega(\xi) = \text{const.}$

for $-\infty < \xi < -1$, but since this part of the real axis corresponds to the sill where $y = \text{Im } G(\phi) = \text{Im } \Omega(\xi)$ is zero the constant of integration is zero so that

$$\text{Im } \Omega(\xi) = 0 , \qquad -\infty < \xi < -1 .$$

This implies that $\Omega(\zeta)$ can be analytically continued across

$$\text{Im } \zeta = 0 , \qquad -\infty < \text{Re } \zeta < -1 ;$$

in accordance with the formula

$$\Omega(\overline{\zeta}) = \overline{\Omega(\zeta)} .$$

Therefore $\Omega(\zeta)$ must be analytic in the cut plane

$$\Lambda: \quad 0 < \arg (\zeta+1) < 2\pi$$

subject to a nonlinear boundary condition along the banks of the cut.

In the beginning the problem was to determine a function $F(z)$ analytic in an unknown domain D but subject to two boundary conditions along each of the unknown parts, Γ_1 and Γ_2, of the boundary of D. We have seen how the dual boundary conditions enable us to transform the problem into one for the determination of a function $\Omega(\zeta)$ analytic in a known domain but subject to one nonlinear boundary condition. The nature of the nonlinearity is such that the probability of finding $\Omega(\zeta)$ in closed form is practically nil.

Aside from a strictly numerical analysis it seems that the best that can be done is equivalent to expressing $\Omega(\zeta)$ as a function which satisfies a nonlinear integral equation and then resorting to some approximation scheme. Various integral equations can be derived depending on the part of the nonlinear boundary condition we think of as known. We proceed to regard the right hand sides of (2.6) and (2.7) as known and derive an integral equation for $\ell n[-\pi\zeta\Omega'(\zeta)]$.

Consider the function $\ell n[\frac{-\pi\zeta\Omega'(\zeta)}{h}]/\sqrt{\zeta+1}$. This function is analytic in Λ; and along $-\infty < \xi < -1$ we have

$$\begin{aligned} \text{Re } \frac{1}{\sqrt{\xi+1}}\, \ell n[\frac{-\pi\xi\Omega'(\xi)}{h}] &= \frac{1}{\sqrt{|\xi+1|}}\, \text{Im } \ell n[\frac{-\pi\xi\Omega'(\xi)}{h}] \\ &= \frac{1}{\sqrt{|\xi+1|}}\, \arg[\frac{-\pi\xi\Omega'(\xi)}{h}] \\ &= 0 \end{aligned}$$

because $\text{Im } \Omega'(\xi) = 0$ for $-\infty < \xi < -1$ and $-\pi\xi\Omega'(\xi) \to a$ as $\xi \to -\infty$. Hence by continuation

$$\frac{1}{\sqrt{\xi-io}}\, \ell n[\frac{-\pi(\xi-io)\Omega'(\xi-io)}{h}] = -\overline{\frac{1}{\sqrt{\xi+io}}\, \ell n[\frac{-\pi(\xi+io)\Omega'(\xi+io)}{h}]}\ .$$

Now an application of the Cauchy integral formula to the slit plane Λ gives

$$\frac{1}{\sqrt{\zeta+1}}\,\ell n[\frac{-\pi\zeta\Omega'(\zeta)}{h}] = \frac{1}{2\pi i}\int_{-1}^{\infty}\frac{1}{\sqrt{\lambda+1}\,(\lambda-\zeta)}\left\{\begin{array}{l}\ell n[\frac{-\pi(\lambda+io)\Omega'(\lambda+io)}{h}] \\ \\ +\ \ell n[\frac{-\pi(\lambda+io)\Omega'(\lambda+io)}{h}]\end{array}\right\}d\lambda$$

or

$$\ell n[\frac{-\pi\zeta\Omega'(\zeta)}{h}] = \frac{\sqrt{\zeta+1}}{\pi i}\int_{-1}^{\infty}\frac{\text{Re}\ \ell n[\frac{-\pi(\lambda+io)\Omega'(\lambda+io)}{h}]}{\sqrt{\lambda+1}\,(\lambda-\zeta)}\,d\lambda\ .$$

Then from the conditions (2.6) and (2.7) we have

$$\begin{aligned}(2.8)\quad \ell n[\frac{-\pi\zeta\Omega'(\zeta)}{h}] = &\frac{i\sqrt{\zeta+1}}{2\pi}\int_{-1}^{0}\frac{\ell n[u^2+2ga(1+\bar{p})-2g\ \text{Im}\,\Omega(\lambda)]}{\sqrt{\lambda+1}\,(\lambda-\zeta)}\,d\lambda \\ &+\frac{i\sqrt{\zeta+1}}{2\pi}\int_{0}^{\infty}\frac{\ell n[u^2+2ga-2g\ \text{Im}\,\Omega(\lambda)]}{\sqrt{\lambda+1}\,(\lambda-\zeta)}\,d\lambda\ .\end{aligned}$$

In the above we have implicitly assumed that $\ell n[-\pi\zeta\Omega'(\zeta)]$ possesses no singularity at $\zeta = -1$. If we introduce

$$\varepsilon = \frac{ga}{u^2}$$

and use

$$\frac{i\sqrt{\zeta+1}}{2\pi}\int_{-1}^{\infty}\frac{d\lambda}{\sqrt{\lambda+1}\,(\lambda-\zeta)} = -\frac{1}{2}$$

then (2.8) becomes

$$\ln\left[\frac{-\pi\zeta\Omega'(\zeta)u}{h}\right] = \frac{i\sqrt{\zeta+1}}{2\pi}\int_{-1}^{0}\frac{\ln\left[1+2\varepsilon(1+\bar{p})-\frac{2\varepsilon}{a}\,\mathrm{Im}\,\Omega(\lambda)\right]}{\sqrt{\lambda+1}\,(\lambda-\zeta)}\,d\lambda$$

$$+\frac{i\sqrt{\zeta+1}}{2\pi}\int_{0}^{\infty}\frac{\ln\left[1+2\varepsilon-\frac{2\varepsilon}{a}\,\mathrm{Im}\,\Omega(\lambda)\right]}{\sqrt{\lambda+1}\,(\lambda-\zeta)}\,d\lambda\ . \tag{2.9}$$

Finally, if we substitute

$$h = au\ ,$$

$$\Omega(\zeta) = ai + a\omega(\zeta)\ ,$$

and use the unit function

$$\mu(t) = \begin{cases} 1 & t > 0 \\ \\ 0 & t < 0\ ; \end{cases}$$

we see that (2.9) can be written as

$$\ln[-\pi\zeta\omega'(\zeta)] = \frac{i\sqrt{\zeta+1}}{2\pi}\int_{-1}^{\infty}\frac{\ln\left[1+2\varepsilon\left[\bar{p}\mu(-\lambda)-\mathrm{Im}\,\omega(\lambda)\right]\right]}{\sqrt{\lambda+1}\,(\lambda-\zeta)}\,d\lambda\ . \tag{2.10}$$

An integral equation for $\omega(\xi)$, $-1 < \xi < \infty$, can now be produced by letting $\zeta \to \xi+i0$. However, we do not need this equation explicitly because we are interested in studying the consequences of the simple and seemingly most natural assumption that $\omega(\zeta)$ possesses the asymptotic expansion

$$\omega(\zeta) = \sum_{n=0}^{\infty}\varepsilon^n\omega_n(\zeta)$$

for small ε and at least $|\zeta| > r > 0$.

3. Terms of the Expansion

The substitution of

$$\Omega(\zeta) = ai + a\omega(\zeta) = ai + a\sum_{n=0}^{\infty} \varepsilon^n \omega_n(\zeta) \tag{3.1}$$

in the boundary conditions (2.5), (2.6) and (2.7) would generate an infinite sequence of boundary value problems which could be solved recursively. This sequence is equivalent to what is found by substituting

$$\omega(\zeta) = \sum_{n=0}^{\infty} \varepsilon^n \omega_n(\zeta) \tag{3.2}$$

in (2.10) and equating coefficients of like powers of ε. The result of doing this gives the following for ω_o, ω_1 and ω_2:

$$\ell n[-\pi\zeta\omega_o'(\zeta)] = 0 \tag{3.3}$$

$$\frac{\omega_1'(\zeta)}{\omega_o'(\zeta)} = \frac{i\sqrt{\zeta+1}}{\pi} \int_{-1}^{\infty} \frac{[\bar{p}\mu(-\lambda) - \operatorname{Im}\, \omega_o(\lambda)]}{\sqrt{\lambda+1}\,(\lambda-\zeta)}\, d\lambda \tag{3.4}$$

$$\frac{\omega_2'(\zeta)}{\omega_o'(\zeta)} - \frac{1}{2}\left[\frac{\omega_1'(\zeta)}{\omega_o'(\zeta)}\right]^2 = -\frac{i\sqrt{\zeta+1}}{\pi} \int_{-1}^{\infty} \frac{\{\operatorname{Im}\, \omega_1(\lambda) + [\bar{p}\mu(-\lambda) - \operatorname{Im}\, \omega_o(\lambda)]^2\}}{\sqrt{\lambda+1}\,(\lambda-\zeta)}\, d\lambda\,. \tag{3.5}$$

It should be noted that since $\Omega(\zeta)$ is analytic in the slit plane Λ, this must also be the case for each $\omega_n(\zeta)$. Moreover, because the

derivative $\omega'(\zeta)$ appears in the integral equation (2.10) we need a side condition to fix $\omega(\zeta)$. Such is provided by our mapping which requires $\zeta = -1$ to correspond to $z = 0$. Hence

$$0 = \Omega(-1) = ai + a \sum_{n=0}^{\infty} \varepsilon^n \omega_n(-1)$$

from which

$$\begin{cases} \omega_0(-1) = -i \\ \omega_n(-1) = 0 , \qquad n \neq 0 . \end{cases} \tag{3.6}$$

Integration of (3.3) yields

$$\omega_0(\zeta) = -\frac{1}{\pi} \ell n\, \zeta \tag{3.7}$$

so that along the real axis

$$\operatorname{Im} \omega_0(\xi) = \begin{cases} -1 & -1 < \xi < 0 \\ 0 & 0 < \xi . \end{cases} \tag{3.8}$$

The function $\omega_0(\zeta)$ corresponds to the sill based jet that could exist if no gravitational force were acting. If g were zero we would have

$$z = \Omega(\zeta) = ai + a\omega_0(\zeta) \tag{3.9}$$

$$= ai - \frac{a}{\pi} \ell n\, \zeta .$$

For $-1 < \xi < 0$, corresponding to the lower nappe, (3.9) gives

(3.10) $$y = \operatorname{Im} z = \operatorname{Im} \Omega(\xi) = a + a \operatorname{Im} \omega_0(\xi) = 0 \ ;$$

and for the upper nappe, corresponding to $0 < \xi < \infty$, (3.9) gives

(3.11) $$y = \operatorname{Im} z = \operatorname{Im} \Omega(\xi) = a \ .$$

the velocity components of the flow (3.9) are

(3.12)
$$\phi_x = \frac{\operatorname{Re} G'(w)}{|G'(w)|^2} = -h \frac{\operatorname{Re} \pi\zeta\Omega'(\zeta)}{|\pi\zeta\Omega'(\zeta)|^2} = \frac{h}{a} = u$$

$$\phi_y = -h \frac{\operatorname{Im} \pi\zeta\Omega'(\zeta)}{|\pi\zeta\Omega'(\zeta)|^2} = 0 \ .$$

These results describe a uniform horizontal flow with velocity u. We are interested in the perturbation of this flow which is caused by gravitational action.

Expansions different from (3.1) can be assumed; for example an expansion parameter different from $\varepsilon = ga/u^2$ is a possibility. Besides, we can contemplate iteration processes for the determination of ω. However, in our expansion, ω_1, as given by (3.4), measures the first order effect of the presence of the gravitational acceleration g. The substitution of (3.7) in (3.4) yields

$$\omega_1'(\zeta) = -\frac{i(\bar{p}+1)\sqrt{\zeta+1}}{\pi^2\zeta} \int_{-1}^{0} \frac{d\lambda}{\sqrt{\lambda+1}\ (\lambda-\zeta)}$$

and after performing the integration

(3.13) $$\omega_1'(\zeta) = -\frac{i(\bar{p}+1)}{\pi^2\zeta} \ln\left(\frac{\sqrt{\zeta+1}-1}{\sqrt{\zeta+1}+1}\right) \ .$$

Since we must have $\omega_1(-1) = 0$, (3.13) gives

$$(3.14) \qquad \omega_1(\zeta) = -\frac{i(\overline{p}+1)}{\pi^2} \int_{-1}^{\zeta} \frac{1}{\lambda} \ell n \left(\frac{\sqrt{\lambda+1}-1}{\sqrt{\lambda+1}+1} \right) d\lambda$$

where the path of integration from -1 to ζ is in the slit plane Λ. As far as we know the integral in (3.14) is neither tabulated nor expressible as a finite combination of tabulated functions. In order to study $\omega_1(\zeta)$ in the neighborhood of various values of ζ without numerical integration it appears that we must resort to several different expansions of (3.14).

The integral in (3.14) can be written

$$\int_{-1}^{\zeta} \frac{1}{\lambda} \ell n \left(\frac{\sqrt{\lambda+1}-1}{\sqrt{\lambda+1}+1} \right) d\lambda = \int_{-1}^{\zeta} \frac{1}{\lambda} [\ell n\, \lambda - 2\, \ell n(\sqrt{\lambda+1}+1)] d\lambda$$

$$= \int_{-1}^{\zeta} \frac{1}{\lambda} (\ell n\, \lambda - 2\, \ell n\, 2) d\lambda - 2 \int_{-1}^{0} \frac{[\ell n(\sqrt{\lambda+1}+1) - \ell n\, 2]}{\lambda} d\lambda$$

$$- 2 \int_{0}^{\zeta} \frac{[\ell n(\sqrt{\lambda+1}+1) - \ell n\, 2]}{\lambda} d\lambda .$$

the value of the definite integral is

$$-2 \int_{-1}^{0} \frac{[\ell n(\sqrt{\lambda+1}+1) - \ell n\, 2]}{\lambda} d\lambda = \int_{0}^{1} \frac{\ell n\, \lambda\, d\lambda}{\sqrt{1-\lambda}\,(\sqrt{1-\lambda}+1)}$$

$$= 2\, \ell n^2 2 - \frac{\pi^2}{6} .$$

For $|\lambda| < 1$ we have

$$2\ \ell n(\sqrt{1+\lambda}+1) - 2\ \ell n\ 2 = -\frac{1}{\sqrt{\pi}} \sum_{k=1}^{\infty} \frac{(-1)^k \Gamma(\frac{1}{2}+k)}{k!} \cdot \frac{\lambda^k}{k} \quad .$$

It follows that for $|\zeta| < 1$ we can express $\omega_1(\zeta)$ in the form

$$(3.15)\quad \omega_1(\zeta) = -\frac{i(\bar{p}+1)}{\pi^2} \left[\begin{array}{l} \frac{1}{2}\ (\ell n\ \zeta - 2\ \ell n\ 2)^2 + \frac{\pi^2}{3} \\ \\ + 2\pi i\ \ell n\ 2 + \frac{1}{\sqrt{\pi}} \sum_{k=1}^{\infty} \frac{(-1)^k \Gamma(\frac{1}{2}+k)}{k!} \cdot \frac{\zeta^k}{k^2} \end{array} \right] .$$

If ζ is in the neighborhood of the origin which corresponds to the flow far downstream from the brink of the overfall, $\omega_1(\zeta)$ behaves like

$$(3.16)\quad \omega_1(\zeta) = -\frac{i(\bar{p}+1)}{\pi^2} \left[\frac{1}{2}(\ell n\ \zeta - 2\ \ell n\ 2)^2 + \frac{\pi^2}{3} + 2\pi i\ \ell n\ 2\right] + o(|\zeta|) \ .$$

The representation (3.14) is equivalent to

$$(3.17)\qquad \omega_1(\zeta) = -\frac{i(\bar{p}+1)}{\pi^2} \left[\begin{array}{l} \int_{-1}^{\infty} \frac{1}{\lambda}\ \ell n\left(\frac{\sqrt{\lambda+1}-1}{\sqrt{\lambda+1}+1}\right) d\lambda \\ \\ -\int_{\zeta}^{\infty} \frac{1}{\lambda}\ \ell n\left(\frac{\sqrt{\lambda+1}-1}{\sqrt{\lambda+1}+1}\right) d\lambda \end{array} \right] .$$

The path of integration for the definite integral is in the slit Λ-plane from -1 to ∞ — it does not pass through the origin. An evaluation shows

$$\int_{-1}^{\infty} \frac{1}{\lambda}\ \ell n\left(\frac{\sqrt{\lambda+1}-1}{\sqrt{\lambda+1}+1}\right) d\lambda = 2\pi i\ \ell n\ 2$$

which means, as we can see from (3.17) that

$$\omega_1(\infty) = \frac{2(\bar{p}+1)}{\pi} \ln 2 .$$

For $|\lambda| > 1$ we have the expansion

$$\ln\left(\frac{\sqrt{\lambda+1}-1}{\sqrt{\lambda+1}+1}\right) = -\frac{1}{\sqrt{\pi}} \sum_{k=0}^{\infty} \frac{(-1)^k \Gamma(\frac{1}{2}+k)}{k!(k+\frac{1}{2})\lambda^{k+\frac{1}{2}}} .$$

Therefore the expansion

$$(3.18)\quad \omega_1(\zeta) = -\frac{i(\bar{p}+1)}{\pi^2}\left[2\pi i \ln 2 + \frac{1}{\sqrt{\pi}} \sum_{k=0}^{\infty} \frac{(-1)^k \Gamma(\frac{1}{2}+k)}{k!(k+\frac{1}{2})^2} \cdot \frac{1}{\zeta^{k+\frac{1}{2}}}\right]$$

is valid for $|\zeta| > 1$.

Using the substitution $\sqrt{\lambda+1} = u$, the representation (3.14) can be changed to

$$\omega_1(\zeta) = -\frac{i(\bar{p}+1)}{\pi^2} \int_0^{\sqrt{\zeta+1}} \frac{2u}{u^2-1} \ln\left(\frac{u-1}{u+1}\right) du$$

which shows that for the neighborhood of $\zeta = -1$, $\omega_1(\zeta)$ can be expanded in powers of $(\zeta+1)^{1/2}$. We find

$$(3.19)\quad \omega_1(\zeta) = -\frac{i(\bar{p}+1)}{\pi^2}\left[i\pi \ln(-\zeta) + 4 \sum_{n=1}^{\infty} \left(\sum_{k=1}^{n} \frac{1}{2k-1}\right) \frac{(\zeta+1)^{\frac{2n+1}{2}}}{2n+1}\right]$$

where the expansion of $\ln(-\zeta)$ has been suppressed.

A power series expansion for the neighborhood of $\zeta = 1$ can be deduced from (3.17). It turns out to be

$$(3.20) \qquad \omega_1(\zeta) = -\frac{i(\overline{p}+1)}{\pi^2}\begin{bmatrix} 2\pi i \ \ell n\ 2 + 3.812 \\ -\ 1.763(\zeta-1) + 1.235(\zeta-1)^2 \\ -\ .779(\zeta-1)^3 \ \ldots \end{bmatrix} .$$

4. First Order Approximation

Before proceeding any further it is of interest to examine in more detail the implications of the first order approximation

$$(4.1) \qquad z = \Omega(\zeta) \sim \Omega_1(\zeta) = ai + a\omega_o(\zeta) + a\varepsilon\omega_1(z) = z_1(\zeta) .$$

This gives the first order flow parametrically in terms of the complex parameter ζ:

$$\frac{x_1(\zeta)}{a} = \mathrm{Re}\left\{ -\frac{1}{\pi}\,\ell n\ \zeta + \varepsilon\omega_1(\zeta)\right\}$$

$$\frac{y_1(\zeta)}{a} = 1 + \mathrm{Im}\left\{ -\frac{1}{\pi}\,\ell n\ \zeta + \varepsilon\omega_1(\zeta)\right\} .$$

The first order shape of the lower nappe in the neighborhood of the brink is given by (3.19) if we take $-1 < \zeta = \xi << 0$. We have

$$\frac{x_1(\xi)}{a} = -\frac{1}{\pi}\ln|\xi| + \frac{\varepsilon(\bar{p}+1)}{\pi}\ln|\xi|$$

$$\frac{y_1(\xi)}{a} = -\frac{\varepsilon(\bar{p}+1)}{\pi^2}\cdot 4\sum_{n=1}^{\infty}\left(\sum_{k=1}^{n}\frac{1}{2k-1}\right)\frac{(1+\xi)^{\frac{2n+1}{2}}}{2n+1}$$

$$= -\frac{4\varepsilon(\bar{p}+1)}{\pi^2}\left[\frac{(1+\xi)^{3/2}}{3} + \frac{4}{15}(1+\xi)^{5/2} + \ldots\right].$$

Our development is based on the assumption that ε is small. Notice that if at this point we try to relax the assumption and suppose that the last result is valid for $\varepsilon = 1$, $\bar{p} = 0$, then we are left with $x_1(\xi)/a = 0$. This is one more example of the complications which usually arise when we investigate critical flows.

The approximate shapes of the first order shapes of the nappes far downstream from the brink come from (3.16). For the lower nappe we have

$$\frac{\widetilde{x_1(\xi)}}{a} = -\frac{\ln|\xi|}{\pi} + \frac{\varepsilon(\bar{p}+1)\ln|\xi|}{\pi}$$

$$\frac{\widetilde{y_1(\xi)}}{a} = -\frac{\varepsilon(\bar{p}+1)}{\pi^2}\left[\frac{1}{2}(\ln|\xi| - 2\ln 2)^2 - \frac{\pi^2}{6}\right]$$

and for the upper nappe we have

$$\frac{\widetilde{x_1(\xi)}}{a} = -\frac{\ln\xi}{\pi} + \frac{\varepsilon(\bar{p}+1)\,2\ln 2}{\pi}$$

$$\frac{\widetilde{y_1(\xi)}}{a} = 1 - \frac{\varepsilon(\bar{p}+1)}{\pi^2}\left[\frac{1}{2}(\ln\xi - 2\ln 2)^2 + \frac{\pi^2}{3}\right].$$

These are parametric equations for the respective parabolas

$$\tilde{y}_1 = \frac{a\varepsilon(\bar{p}+1)}{6} - \frac{\varepsilon(\bar{p}+1)}{2a[\varepsilon(\bar{p}+1) - 1]^2} \cdot \left\{ \tilde{x}_1 - \frac{2a}{\pi} [\varepsilon(\bar{p}+1) - 1] \ln 2 \right\}^2$$

and

$$\tilde{y}_1 = a - \frac{a\varepsilon(\bar{p}+1)}{3} - \frac{\varepsilon(\bar{p}+1)}{2a} \left\{ \tilde{x}_1 - \frac{2a}{\pi} [\varepsilon(\bar{p}+1) - 1] \ln 2 \right\}^2 .$$

As the same coordinate $\tilde{y}_1$ decreases to $-\infty$ the magnitude of the difference of the abscissas of the parabolas increases, that is, they diverge. Since this is contrary to the observed behavior of the nappes of a waterfall, the parabolas should not be accepted as good approximations particularly when $\varepsilon = ga/u^2$ is not small. However, if we take the case for which the pressures on the nappes are the same ($\bar{p} = 0$) and let $a \to 0$ we find that each parabola reduces to

$$\tilde{y}_1 = - \frac{g\tilde{x}_1^2}{2u^2}$$

which gives the shape of a thin heavy sheet of fluid projected horizontally from the brink with velocity u and subject to equal pressures on its faces.

It can be seen from (3.17) that for the upper nappe, where $0 < \xi$,

$$\frac{x_1(\xi)}{a} = - \frac{1}{\pi} \ln \xi + \frac{\varepsilon(\bar{p}+1)}{\pi} 2 \ln 2$$

and

$$\frac{y_1(\xi)}{a} = 1 + \frac{\varepsilon(\bar{p}+1)}{\pi^2} \int_{\xi}^{\infty} \frac{1}{\lambda} \ell n \left(\frac{\sqrt{\lambda+1} - 1}{\sqrt{\lambda+1} + 1} \right) d\lambda \ .$$

The first order ratio of brink depth to depth upstream at ∞ is given by

$$\frac{y_1(\xi_o)}{a} = 1 + \frac{\varepsilon(\bar{p}+1)}{\pi^2} \int_{\xi_o}^{\infty} \frac{1}{\lambda} \ell n \left(\frac{\sqrt{\lambda+1} - 1}{\sqrt{\lambda+1} + 1} \right) d\lambda \tag{4.2}$$

where

$$\ell n \ \xi_o = \varepsilon(\bar{p}+1) \ 2 \ \ell n \ 2 \ .$$

We cannot expect the formula (4.2) to be very accurate if $\varepsilon = ga/u^2$ is not small. However, it is interesting to see what (4.2) gives if $\bar{p} = 0$ and the velocity far upstream is critical so that $\varepsilon = 1$. For these conditions, which prevail in many engineering analyses of transition from channel flow to overfall, our first order approximation gives

$$\xi_o = 4$$

and

$$\frac{y_1(\xi_o)}{a} = 1 + \frac{1}{\pi^2} \int_{4}^{\infty} \frac{1}{\lambda} \ell n \left(\frac{\sqrt{1+\lambda} - 1}{\sqrt{1+\lambda} + 1} \right) d\lambda$$

$$= 1 - \frac{1}{\pi^2} \frac{1}{\sqrt{\pi}} \sum_{k=0}^{\infty} \frac{(-1)^k \Gamma(\frac{1}{2}+k)}{k!(k+\frac{1}{2})^2} \cdot \frac{1}{4^{k+\frac{1}{2}}}$$

$$= 1 - \frac{1}{\pi^2} \left[2 - \frac{1}{30} + \frac{3}{1600} \cdots \right]$$

$$\simeq .80 \ .$$

This is to be compared with the value

$$\frac{y_1}{a} = .71$$

which is the average of contraction coefficient values

.715	Rouse [1]
.705	Southwell and Vaisey [2]
.720	Jaeger [3]
.720	Roy [4]
.710	Fraser [5]
.676	Hay and Markland [6]

deduced from various experimental and mathematical approximation procedures different from the one we are using.

Physical consideration of the decreasing slope of the upper nappe streamline of an overfall from 0 to $-\infty$; and consideration of our choice of mapping to the complex w-plane, where $\phi = 0$ corresponds to the brink, together show that the point on the upper nappe directly above the brink must also be a point on the potential curve

$$\phi(x,y) = -\gamma \ , \qquad \gamma > 0 \ .$$

This point corresponds to a point $\zeta = \xi \geq 1$ because

$$\zeta = -e^{-\frac{\pi w}{h}} = -e^{-\frac{\pi}{h}(-\gamma+ih)}$$

$$= e^{\frac{\pi\gamma}{h}} \geq 1 \ .$$

If we substitute $\xi_0 = 1$ in (4.2) we find

$$\frac{y_1(1)}{a} = 1 - \frac{1}{\pi^2}\left[4 - \frac{2}{9} + \frac{3}{50} - \frac{5}{196} \cdots\right]$$

$$\simeq .62$$

a value which is presumably too low. It is amusing to notice that the mean of this value .62 and .80 is .71.

5. Second Order Term

We turn now to a study of the second order term $\omega_2(\zeta)$ of the expansion (3.1). This term is defined by (3.5), namely,

$$(5.1)\quad \frac{\omega_2'(\zeta)}{\omega_0'(\zeta)} = \frac{1}{2}\left[\frac{\omega_1'(\zeta)}{\omega_0'(\zeta)}\right]^2 - \frac{i\sqrt{\zeta+1}}{\pi}\int_{-1}^{\infty} \frac{\{\operatorname{Im}\,\omega_1(\lambda) + [\overline{p\mu}(-\lambda) - \operatorname{Im}\,\omega_0(\lambda)]^2\}}{\sqrt{\lambda+1}\,(\lambda-\zeta)}\,d\lambda\,.$$

Substitution of the now known $\omega_0(\zeta)$ and $\omega_1(\zeta)$ gives

$$(5.2)\quad \omega_2'(\zeta) = \frac{(\overline{p}+1)^2}{2\pi^3\zeta}\,\ell n^2\left(\frac{\sqrt{\zeta+1}-1}{\sqrt{\zeta+1}+1}\right) - (\overline{p}+1)\omega_1'(\zeta) + \frac{i\sqrt{\zeta+1}}{\pi^2\zeta}\int_{-1}^{\infty} \frac{\operatorname{Im}\,\omega_1(\lambda)d\lambda}{\sqrt{\lambda+1}\,(\lambda-\zeta)}$$

which holds for $\operatorname{Im}\,\zeta > 0$. Since $\operatorname{Im}\,\omega_1(\xi) = 0$ for $\xi < -1$; the

function $\omega_1(\zeta)$ is analytic in Λ, the slit ζ-plane, and such that $\omega_1(\xi-io) = \overline{\omega_1(\xi+io)}$ for $-1 < \xi < \infty$. Also

$$\omega_1(\infty) = \frac{2(\bar{p}+1)\ \ell n\ 2}{\pi}\ , \tag{5.3}$$

as given in Section 3, is real. Hence equation (5.2) can be written

$$\omega_2'(\zeta) = \frac{(\bar{p}+1)^2}{2\pi^3\zeta}\ \ell n^2\left(\frac{\sqrt{\zeta+1}-1}{\sqrt{\zeta+1}+1}\right) - (\bar{p}+1)\omega_1'(\zeta)$$

$$+ \frac{\sqrt{\zeta+1}}{2\pi^2\zeta}\int_{-1}^{\infty}\frac{[\omega_1(\lambda+io)-\omega_1(\infty)]}{\sqrt{\lambda+io+1}\ (\lambda-\zeta)}\,d\lambda$$

$$+ \frac{\sqrt{\zeta+1}}{2\pi^2\zeta}\int_{-1}^{\infty}\frac{[\omega_1(\lambda-io)-\omega_1(\infty)]}{\sqrt{\lambda-io+1}\ (\lambda-\zeta)}\,d\lambda$$

where the paths in the integrals are along the upper and lower banks of the cut along the real axis of the ζ-plane from -1 to $+\infty$. A deformation of these paths into the remainder of the real axis yields

$$\omega_2'(\zeta) = \frac{(\bar{p}+1)^2}{2\pi^3\zeta}\ \ell n^2\left(\frac{\sqrt{\zeta+1}-1}{\sqrt{\zeta+1}+1}\right) - (\bar{p}+1)\omega_1'(\zeta) \tag{5.4}$$

$$+ \frac{i[\omega_1(\zeta)-\omega_1(\infty)]}{\pi\zeta} + \frac{\sqrt{\zeta+1}}{\pi^2\zeta}\int_{-1}^{-\infty}\frac{[\omega_1(\lambda)-\omega_1(\infty)]}{\sqrt{\lambda+1}\ (\lambda-\zeta)}\,d\lambda\ .$$

Integration of (5.4) gives

$$(5.5)\quad \omega_2(\zeta) - \omega_2(\infty) = -\frac{(\bar{p}+1)^2}{2\pi^3}\int_{\zeta}^{\infty}\frac{1}{\sigma}\ln^2\left(\frac{\sqrt{\sigma+1}-1}{\sqrt{\sigma+1}+1}\right)d\sigma$$

$$-(\bar{p}+1)[\omega_1(\zeta)-\omega_1(\infty)] - \frac{1}{\pi}\int_{\zeta}^{\infty}\frac{[\omega_1(\sigma)-\omega_1(\infty)]}{\sigma}\,d\sigma$$

$$+\frac{1}{\pi^2}\int_{-1}^{-\infty}\frac{[\omega_1(\lambda)-\omega_1(\infty)]}{\sqrt{\lambda+1}}\left\{\begin{array}{l}\dfrac{1}{\lambda}\ln\dfrac{\sqrt{\zeta+1}-1}{\sqrt{\zeta+1}+1} - \dfrac{\pi\sqrt{-\lambda-1}}{\lambda}\\[2ex] +\dfrac{2\sqrt{-\lambda-1}}{\lambda}\arctan\dfrac{\sqrt{\zeta+1}}{\sqrt{-\lambda-1}}\end{array}\right\}d\lambda\ .$$

In order to go on with the exposition of $\omega_2(\zeta)$ we need the values of some definite integrals. These integrals are listed in the appendix with indications of methods for their evaluation.

Recalling that $\omega_2(-1) = \omega_1(-1) = 0$, we see that for $\zeta = -1$, (5.5) becomes

$$\omega_2(\infty) = \frac{(\bar{p}+1)^2}{2\pi^3}\int_{-1}^{\infty}\frac{1}{\sigma}\ln^2\left(\frac{\sqrt{\sigma+1}-1}{\sqrt{\sigma+1}+1}\right)d\sigma - (\bar{p}+1)\omega_1(\infty)$$

$$-\frac{1}{\pi}\int_{-1}^{-\infty}\frac{[\omega_1(\lambda)-\omega_1(\infty)]}{\lambda\sqrt{\lambda+1}}\,d\lambda\ .$$

A reference to the definite integrals tabulated in the appendix shows that the value of $\omega_2(\zeta)$ at infinity in the Λ-plane is

$$(5.6)\quad \omega_2(\infty) = -\frac{(\bar{p}+1)^2}{\pi}\,3\ln 2 + \frac{(\bar{p}+1)^2}{2\pi^3}(8.416) + \frac{(\bar{p}+1)}{\pi^3}(8.416)\ .$$

The shape of the upper nappe depends on the behavior of $\omega_2(\zeta)$ for $\zeta = \xi > 0$. From (5.5) we find that the real part of $\omega_2(\xi)$ for $\xi > 0$ is

$$(5.7) \qquad \text{Re } \omega_2(\xi) = -\frac{(\bar{p}+1)^2}{2\pi^3} \int_{\xi}^{\infty} \frac{1}{\sigma} \ell n^2 \left(\frac{\sqrt{\sigma+1}-1}{\sqrt{\sigma+1}+1} \right) d\sigma + \frac{1}{\pi} \int_{\xi}^{\infty} \frac{\text{Im } \omega_1(\sigma) d\sigma}{\sigma} + \omega_2(\infty) .$$

The point $\xi = 1$ corresponds to a point in the neighborhood of $(0,b)$ where b is the brink depth in the physical plane of flow. For the neighborhood of $\xi = 1$ the Taylor expansion of (5.7) is

$$(5.8) \qquad \text{Re } \omega_2(\xi) = \omega_2(\infty) - \frac{(\bar{p}+1)^2}{2\pi^3} \left[3.512 - 3.108(\xi-1) + 2.800(\xi-1)^2 - 1.327(\xi-1)^3 \ldots \right] - \frac{(\bar{p}+1)}{\pi^3} \left[7.869 - 3.812(\xi-1) + 2.788(\xi-1)^2 - 2.270(\xi-1)^3 \ldots \right] .$$

The imaginary part of $\omega_2(\xi)$ for $\xi > 0$ is

$$(5.9)\qquad \operatorname{Im}\omega_2(\xi) = -(\bar{p}+1)\operatorname{Im}\omega_1(\xi) + \frac{(\bar{p}+1)(8.416)}{\pi^4}\,\ell n\left(\frac{\sqrt{\xi+1}-1}{\sqrt{\xi+1}+1}\right)$$

$$- \frac{(\bar{p}+1)}{\pi^2}\left[2\,\ell n^2 2 + \frac{\pi^2}{6}\right]$$

$$- \frac{2}{\pi^2}\int_1^{\infty} \frac{[\omega_1(-\lambda)-\omega_1(\infty)]}{\lambda}\,\arctan\frac{\sqrt{\xi+1}}{\sqrt{\lambda-1}}\,d\lambda\ .$$

Useful upper and lower bounds can be found for $\operatorname{Im}\omega_2(\xi)$ if we use the inequality (A.7) in the appendix. If $(\bar{p}+1) > 0$ we find

$$(5.10)\qquad \operatorname{Im}\omega_2(\xi) < -(\bar{p}+1)\operatorname{Im}\omega_1(\xi) + \frac{(\bar{p}+1)(8.416)}{\pi^4}\,\ell n\left(\frac{\sqrt{\xi+1}-1}{\sqrt{\xi+1}+1}\right)$$

$$- \frac{16(\bar{p}+1)}{\pi^4}\,\frac{1}{\sqrt{\xi}}\,\ell n\,(\sqrt{1+\xi}+\sqrt{\xi})$$

and

$$(5.11)\qquad \operatorname{Im}\omega_2(\xi) > -(\bar{p}+1)\operatorname{Im}\omega_1(\xi) + \frac{(\bar{p}+1)(8.416)}{\pi^4}\,\ell n\left(\frac{\sqrt{\xi+1}-1}{\sqrt{\xi+1}+1}\right)$$

$$- \frac{16(\bar{p}+1)}{\pi^4}\,\frac{1}{\sqrt{\xi}}\,\ell n\,(\sqrt{1+\xi}+\sqrt{\xi}) - .00597(\bar{p}+1)\ .$$

The shape of the lower nappe in the neighborhood of the brink depends on the behavior of $\omega_2(\zeta)$ for $\zeta = \xi$ near $\xi = -1$. An integration of (5.4) shows that for $-1 < \xi < 0$

$$\omega_2(\xi) = \frac{(\bar{p}+1)^2}{2\pi^3} \int_{-1}^{\xi} \frac{1}{\sigma} \ell n^2 \left(\frac{\sqrt{\sigma+1} - 1}{\sqrt{\sigma+1} + 1} \right) d\sigma - (\bar{p}+1)\omega_1(\xi)$$

$$+ \frac{i}{\pi} \int_{-1}^{\xi} \frac{[\omega_1(\sigma) - \omega_1(\infty)]}{\sigma} d\sigma$$

$$+ \frac{1}{\pi^2} \int_{-1}^{-\infty} \frac{[\omega_1(\lambda) - \omega_1(\infty)]}{\sqrt{\lambda+1}} \left\{ \begin{array}{l} \frac{1}{\lambda} \ell n \left(\frac{1 - \sqrt{\xi+1}}{1 + \sqrt{\xi+1}} \right) \\ \\ + \frac{2\sqrt{-\lambda-1}}{\lambda} \arctan \frac{\sqrt{\xi+1}}{\sqrt{-\lambda-1}} \end{array} \right\} d\lambda \ .$$

The real part of $\omega_2(\xi)$ for $-1 < \xi < 0$ is

$$(5.12) \quad \text{Re } \omega_2(\xi) = - \frac{3(\bar{p}+1)^2}{2\pi} \ell n \ (-\xi) + \frac{(\bar{p}+1)^2}{2\pi^3} \int_{-1}^{\xi} \frac{1}{\sigma} \ell n \left(\frac{1 - \sqrt{\sigma+1}}{1 + \sqrt{\sigma+1}} \right) d\sigma$$

$$+ \frac{(\bar{p}+1)}{\pi^3} \int_{-1}^{\xi} \frac{4}{\sigma} \sum_{n=1}^{\infty} \left(\sum_{k=1}^{n} \frac{1}{2k-1} \right) \frac{(\sigma+1)^{(2n+1)/2}}{2n+1} d\sigma$$

which can be expanded into

$$(5.13) \quad \text{Re } \omega_2(\xi) = - \frac{3(\bar{p}+1)^2}{2\pi} \ell n \ (-\xi)$$

$$- \frac{2(\bar{p}+1)^2}{\pi^3} \left[\frac{(\xi+1)^2}{2} + \frac{5}{9}(\xi+1)^3 + \frac{49}{90}(\xi+1)^4 \ \ldots \right]$$

$$- \frac{4(\bar{p}+1)}{\pi^3} \left[\frac{2}{15}(\xi+1)^{5/2} + \frac{6}{35}(\xi+1)^{7/2} + \frac{172}{945}(\xi+1)^{9/2} \ldots \right]$$

valid for $-1 < \xi < 0$.

The imaginary part of $\omega_2(\xi)$ for $-1 < \xi < 0$ is

$$(5.14)\quad \operatorname{Im}\omega_2(\xi) = -2(\bar{p}+1)\operatorname{Im}\omega_1(\xi)$$

$$+\frac{(\bar{p}+1)}{2\pi^2}\ln(-\xi)\,[\ln(-\xi) - 4\ln 2]$$

$$+\frac{(\bar{p}+1)}{\pi^4}(8.416)\ln\left(\frac{1-\sqrt{\xi+1}}{1+\sqrt{\xi+1}}\right)$$

$$-\frac{2}{\pi^2}\int_1^{\infty}\frac{[\omega_1(-\lambda)-\omega_1(\infty)]}{\lambda}\arctan\frac{\sqrt{\xi+1}}{\sqrt{\lambda-1}}\,d\lambda\ .$$

From the inequality (A.7) we find that if $(\bar{p}+1) > 0$ then

$$(5.15)\quad \operatorname{Im}\omega_2(\xi) < I(\xi) - \frac{16(\bar{p}+1)}{\pi^4}\frac{1}{\sqrt{\xi}}\ln(\sqrt{1+\xi}+\sqrt{\xi})$$

$$+\frac{(\bar{p}+1)}{\pi^2}\left[2\ln^2 2 + \frac{\pi^2}{6}\right]$$

and

$$(5.16)\quad \operatorname{Im}\omega_2(\xi) > I(\xi) - \frac{16(\bar{p}+1)}{\pi^4}\frac{1}{\sqrt{\xi}}\ln(\sqrt{1+\xi}+\sqrt{\xi})$$

$$+\frac{(\bar{p}+1)}{\pi^2}\left[2\ln^2 2 + \frac{\pi^2}{6}\right] - (.00597)(\bar{p}+1)\ ;$$

where

$$I(\xi) = -2(\bar{p}+1)\operatorname{Im}\omega_1(\xi)$$

$$+\frac{(\bar{p}+1)}{2\pi^2}\ln(-\xi)\,[\ln(-\xi) - 4\ln 2]$$

$$+\frac{(\bar{p}+1)}{\pi^4}(8.416)\ln\left(\frac{1-\sqrt{1+\xi}}{1+\sqrt{1+\xi}}\right)\ .$$

If we are interested in studying the shapes of the nappes far from the brink we need to know the behavior of $\omega_2(\zeta)$ as $\zeta \to 0$. By using (5.5) and the integrals listed in the appendix we find

$$(5.17)\quad \omega_2(\zeta) = -\frac{(\bar{p}+1)^2}{\pi}\, 3\,\ell n\, 2 + \frac{(\bar{p}+1)^2(8.416)}{2\pi^3} + \frac{(\bar{p}+1)(8.416)}{\pi^3}$$

$$- \frac{(\bar{p}+1)^2}{2\pi^3}\left[-\frac{1}{3}(\ell n\, \zeta - 2\,\ell n\, 2)^3 + 4.808\right]$$

$$+ \frac{i(\bar{p}+1)^2}{2\pi^2}\left[(\ell n\, \zeta - 2\,\ell n\, 2)^2 + \frac{2\pi^2}{3}\right]$$

$$+ \frac{(\bar{p}+1)}{6\pi^3}\left[2\pi^2(\ell n\, \zeta - 2\,\ell n\, 2) + (\ell n\, \zeta - 2\,\ell n\, 2)^3 - 12(1.202057)\right]$$

$$+ \frac{i(\bar{p}+1)(8.416)}{\pi^4}(\ell n\, \zeta - 2\,\ell n\, 2) - \frac{i(\bar{p}+1)}{6} + o(|\zeta|)\ .$$

For the lower nappe with $\bar{p} = 0$ (5.17) reduces to

$$\omega_2(\xi) = -\frac{3\,\ell n\, 2}{\pi} - \frac{.600}{\pi^3}$$

$$+ \frac{1}{3\pi^3}\left[(\ell n\, |\xi| - 2\,\ell n\, 2)^3 - 5\pi^2(\ell n\, |\xi| - 2\,\ell n\, 2)\right]$$

$$+ i\left[-\frac{1}{3} + \frac{8.416}{\pi^4}(\ell n\, |\xi| - 2\,\ell n\, 2) + \frac{3}{2\pi^2}(\ell n\, |\xi| - 2\,\ell n\, 2)^2\right] + o(\xi)\ .$$

It will be recalled that for $\bar{p} = 0$, and $\varepsilon = 1$, $\tilde{x}_1(\xi)$ vanishes for the lower nappe. This is not the case here for Re $\omega_2(\xi)$.

6. Second Order Approximation. Brink Depth

We propose now to see what the second order approximation

$$(6.1) \quad z - \Omega(\zeta) \sim \Omega_2(\zeta) = a\zeta + a\omega_0(\zeta) + a\omega_1(\zeta) + a\varepsilon^2\omega_2(\zeta) = z_2(\zeta)$$

implies with respect to the brink depth b of the overfall. The contraction coefficient b/a is of considerable interest because it appears in various formulae for flow measurement when the overfall is used as a metering device. When the overfall exists in a channel the upstream flow is nearly critical and hence the contraction coefficient for critical flow is particularly interesting.

Our previous results for ω_0, ω_1 and ω_2 show that the parametric equations for the upper nappe corresponding to the neighborhood of $\zeta = 1$ are

$$(6.2) \quad \frac{x_2(\zeta)}{a} = \mathrm{Re}\,\{\omega_0(\zeta) + \varepsilon\omega_1(\xi) + \varepsilon^2\omega_2(\xi)\}$$

$$= -\frac{1}{\pi}\ln\xi + \frac{\varepsilon(\bar{p}+1)}{\pi}\,2\ln 2$$

$$+ \varepsilon^2\left[\frac{(\bar{p}+1)^2}{\pi}\,3\ln 2 + \frac{(\bar{p}+1)^2(8.416)}{2\pi^3} + \frac{(\bar{p}+1)(8.416)}{\pi^3}\right]$$

$$- \frac{\varepsilon^2(\bar{p}+1)^2}{2\pi^3}\left[3.512 - 3.108(\xi-1) + 2.800(\xi-1)^2 - 1.327(\xi-1)^3 \ldots\right]$$

$$- \frac{\varepsilon^2(\bar{p}+1)}{\pi^3}\left[7.869 - 3.812(\xi-1) + 2.788(\xi-1)^2 - 2.270(\xi-1)^3 \ldots\right]$$

and

$$(6.3)\quad \frac{y_2(\xi)}{a} = 1 + \mathrm{Im}\{\omega_o(\xi) + \varepsilon\omega_1(\xi) + \varepsilon^2\omega_2(\xi)\}$$

$$= 1 - \frac{(\bar{p}+1)}{\pi^2}[\varepsilon - \varepsilon^2(\bar{p}+1)]\left[\begin{array}{l} 3.812 - 1.763(\xi-1) \\ \\ + 1.235(\xi-1)^2 - .779(\xi-1)^3 \ldots \end{array}\right]$$

$$+ \frac{\varepsilon^2(\bar{p}+1)(8.416)}{\pi^4}\,\ell n\left(\frac{\sqrt{\xi+1}-1}{\sqrt{\xi+1}+1}\right)$$

$$- \frac{\varepsilon^2 16(\bar{p}+1)}{\pi^4\sqrt{\xi}}\,\ell n\,(\sqrt{1+\xi}+\sqrt{\xi}) - (.00597)\varepsilon^2(\bar{p}+1)\theta$$

where θ is real such that $0 < \theta < 1$ if $(\bar{p}+1) > 0$. In this section we confine ourselves to a discussion of the case for which $\bar{p} = 0$. For this case the upper nappe in the neighborhood of $\xi = 1$ is given by

$$(6.4)\quad \frac{x_2(\xi)}{a} = -\frac{\ell n\ \xi}{\pi} + \frac{\varepsilon\, 2\ \ell n\ 2}{\pi} + \varepsilon^2\left[-\frac{3\ \ell n\ 2}{\pi} + \frac{12.624}{\pi^3}\right]$$

$$- \frac{\varepsilon^2}{\pi^3}\left[\begin{array}{l} 9.625 - 5.364(\xi-1) + 4.188(\xi-1)^2 \\ \\ - 2.934(\xi-1)^3 \ldots \end{array}\right]$$

and

$$(6.5)\quad \frac{y_2(\xi)}{a} = 1 - \frac{(\varepsilon-\varepsilon^2)}{\pi^2}\left[\begin{array}{l} 3.812 - 1.763(\xi-1) \\ \\ + 1.235(\xi-1)^2 - .779(\xi-1)^3 \ldots \end{array}\right]$$

$$+ \frac{\varepsilon^2(8.416)}{\pi^4}\,\ell n\left(\frac{\sqrt{\xi+1}-1}{\sqrt{\xi+1}+1}\right) - \frac{\varepsilon^2 16}{\pi^4\sqrt{\xi}}\,\ell n\,(\sqrt{1+\xi}+\sqrt{\xi})$$

$$- (.00597)\varepsilon^2\theta\ .$$

If we suppose that (6.4) and (6.5) remain good approximations when the parameter ε, which we assumed to be small, is replaced by $\varepsilon = 1$, corresponding to critical flow, then

$$\frac{y_2(1)}{a} = 1 + \frac{8.416}{\pi} \ell n\left(\frac{\sqrt{2}-1}{\sqrt{2}+1}\right) - \frac{16}{\pi^4} \ell n\,(\sqrt{2}+1) - (.00597)\theta$$

$$= .702 - (.006)\theta \,, \qquad 0 < \theta < 1 \,.$$

This is close to the average value .71 noted in Section 4. The acceptance of $b = a[.702 - (.006)\theta]$ as an approximation to the brink depth is tantamount to the assumption that $x_2(1)$ is close to zero. This kind of assumption is implicit in some of the analyses which have been devised for the calculation of b, see for example, Roy [4]. Consequently, such analyses really give an approximate ordinate of a point (α, b_1) on the upper nappe without an estimate of the presumably small abscissa α. According to our second order approximation, $b = a[.702 - (.006)\theta]$ is the depth at

$$x_2(1) = \frac{a}{\pi}\left[-\ell n\ 2 + \frac{3}{\pi^2}\right]$$

$$= -\ .14a \,.$$

In general, if ε is prescribed we can invert (6.4) to find ξ_o such that $x_2(\xi_o) = 0$. The approximation to the contraction coefficient can then be found by substituting ξ_o in (6.5) in order to obtain $y_2(\xi_o)/a$. An estimate of the brink depth can also be found by substituting various values of ξ near $\xi = 1$ in (6.4) and (6.5). For example, take $\varepsilon = .9$ which means that the flow is

supercritical to the extent that $u = \frac{\sqrt{10}}{3}\sqrt{ga} = 1.05\sqrt{ga}$. For this value of ε we have

$$(6.6)\quad \frac{x_2(\xi)}{a} = \frac{1}{\pi}\left\{\begin{array}{l} -(\xi-1) + \frac{(\xi-1)^2}{2} - \frac{(\xi-1)^3}{3} \ldots \\ +.596 \\ -.082[9.625 - 5.364(\xi-1) + 4.188(\xi-1)^2 \ldots] \end{array}\right\}$$

and

$$(6.7)\quad \frac{y_2(\xi)}{a} = 1 - .009[3.812 - 1.763(\xi-1) + 1.235(\xi-1)^2 \ldots]$$

$$+ .070\ \ell n\left(\frac{\sqrt{\xi+1}-1}{\sqrt{\xi+1}+1}\right) - \frac{.133}{\sqrt{\xi}}\ \ell n\left(\sqrt{1+\xi} + \sqrt{\xi}\right) - (.005)\theta\ .$$

Computation shows that for

$$\overline{p} = 0\ , \qquad \varepsilon = .9$$

we have

$$\frac{x_2(1)}{a} = -.061\ , \qquad \frac{y_2(1)}{a} = .725 - (.005)\theta$$

$$\frac{x_2(.9)}{a} = -.044\ , \qquad \frac{y_2(.9)}{a} = .709 - (.005)\theta$$

$$\frac{x_2(.8)}{a} = -.026\ , \qquad \frac{y_2(.8)}{a} = .692 - (.005)\theta\ , \qquad 0 < \theta < 1\ .$$

A comparison of these figures, and others we have obtained in this section, with the values noted in Section 4 indicates that the approximations (6.4) and (6.5) are rather good even for values of ε close to 1.

7. Second Order Approximation. Equations for Shapes of Nappes

We have already seen in Section 6 how the approximate shape of the upper nappe above the brink can be found. In a similar way the second order shape of the lower nappe in the neighborhood of the brink can be obtained by using the parametric equations

$$\frac{x_2(\xi)}{a} = \mathrm{Re}\ \{\omega_o(\xi) + \varepsilon\omega_1(\xi) + \varepsilon^2\omega_2(\xi)\}$$

(7.1)

$$\frac{y_2(\xi)}{a} = 1 + \mathrm{Im}\ \{\omega_o(\xi) + \varepsilon\omega_1(\xi) + \varepsilon^2\omega_2(\xi)\}$$

where ξ is restricted to $-1 < \xi < 0$. Collecting previous results for ω_o, ω_1 and ω_2 we find that for the neighborhood of the brink where $\xi = -1$ the coordinates of the lower nappe are given by

$$\frac{x_2(\xi)}{a} = -\frac{\ell n\ |\xi|}{\pi} + \frac{\varepsilon(\bar{p}+1)\ell n\ |\xi|}{\pi} \tag{7.2}$$

$$+ \varepsilon^2 \left\{ \begin{array}{l} -\dfrac{3(\bar{p}+1)^2 \ell n\ |\xi|}{2\pi} \\ -\dfrac{2(\bar{p}+1)^2}{\pi^3}\left[\dfrac{(\xi+1)^2}{2} + \dfrac{5}{9}(\xi+1)^3 \ldots\right] \\ -\dfrac{4(\bar{p}+1)}{\pi^3}\left[\dfrac{2}{15}(\xi+1)^{5/2} + \dfrac{6}{35}(\xi+1)^{7/2} \ldots\right] \end{array} \right\}$$

and

$$(7.3)\quad \frac{y_2(\xi)}{a} = -\frac{4\varepsilon(\bar{p}+1)}{\pi^2}\left[1+2\varepsilon(\bar{p}+1)\right]\sum_{n=1}^{\infty}\left(\sum_{k=1}^{n}\frac{1}{2k-1}\right)\frac{(\xi+1)^{\frac{2n+1}{2}}}{2n+1}$$

$$+\varepsilon^2\left\{\begin{array}{l}\dfrac{(\bar{p}+1)}{2\pi^2}\,\ell n\,|\xi|\,\left[\ell n\,|\xi| - 4\,\ell n\,2\right]\\[2ex] +\dfrac{(\bar{p}+1)(8.416)}{\pi^4}\,\ell n\left(\dfrac{1-\sqrt{1+\xi}}{1+\sqrt{1+\xi}}\right)\\[2ex] -\dfrac{16(\bar{p}+1)}{\pi^4}\,\dfrac{1}{\sqrt{|\xi|}}\,\ell n\,(\sqrt{1+\xi}+\sqrt{|\xi|})\\[2ex] +\dfrac{(\bar{p}+1)}{\pi^2}\,(2\,\ell n^2\,2+\dfrac{\pi^2}{6}) - (.00597)(\bar{p}+1)\theta\end{array}\right\}$$

where θ is a real number such that $0 < \theta < 1$.

The shapes of the nappes downstream corresponding to the neighborhood of $\xi = 0$ come from combining (3.7), (3.16) and (5.17) and they are given by the complex form

$$(7.4)\quad z_2(\xi) = ai - \frac{a\tau}{\pi} - \frac{a\ 2\ \ell n\ 2}{\pi} - \frac{a\varepsilon i(\bar{p}+1)}{2\pi^2}\left[\tau^2+\frac{2\pi^2}{3}+2\pi i\,\ell n\,2\right]$$

$$+a\varepsilon^2\left\{\begin{array}{l}\dfrac{(\bar{p}+1)^2\ 3\ \ell n\ 2}{\pi}+\dfrac{(\bar{p}+1)^2(8.416)}{2\pi^3}+\dfrac{(\bar{p}+1)(8.416)}{\pi^3}\\[2ex] +\dfrac{(\bar{p}+1)^2}{6\pi^3}[\tau^3-14.424]+\dfrac{i(\bar{p}+1)^2}{2\pi^2}(\tau^2+\dfrac{2\pi^2}{3})\\[2ex] +\dfrac{(\bar{p}+1)}{6\pi^3}\,(2\pi^2\tau+\tau^3-14.424)\\[2ex] +\dfrac{i(\bar{p}+1)(8.416)\tau}{\pi^4}-\dfrac{i(\bar{p}+1)}{6}+o(|\xi|)\end{array}\right\}$$

where we have used τ to denote

$$\tau = \ell n\, \xi - 2\, \ell n\, 2 \ .$$

The upper nappe corresponds to positive values of ξ while the lower nappe corresponds to negative values of ξ. Note that for the upper nappe τ is real and negative, while for the lower nappe

$$\tau = i\pi + \frac{\ell n\, |\xi|}{4}$$

with real part negative. We can expect (7.4) to be a good approximation if ε is small. However, the approximation is not good when $\overline{p} = 0$ and $\varepsilon = 1$. Analysis shows that the breakdown in accuracy for this case is due to the disappointing circumstance that the quadratic terms involving τ^2 cancel out of (7.4).

It is interesting to see what (7.4) implies when we allow a to approach zero so that the overfall degenerates into a sheet. In order to maintain a constant mass flow as $a \to 0$ the velocity u must be taken so that $au\delta = \delta h$ is constant. Then, if we set

$$\tilde{p} = \frac{p_2 - p_1}{\delta h} \ ; \qquad \sigma = -\frac{a\tau}{\pi u}$$

we find that as $a \to 0$ the real and imaginary parts of (7.4) become

$$x_2(\xi) = u\sigma - \tilde{p}(\tilde{p}u + g)\,\frac{\sigma^3}{6}$$

(7.5)

$$y_2(\xi) = -(\tilde{p}u + g)\,\frac{\sigma^2}{2}$$

after retaining dominant terms. Now it can be verified independently of what appears in this paper that in the first stages of fall the

shape of a thin overfall, subject to gravitational attraction and different constant pressures on its faces, is given by

$$
\begin{aligned}
x &= \frac{(g + \tilde{p}u)}{\tilde{p}^2} \sin \tilde{p}t - \frac{gt}{\tilde{p}} \\
y &= \frac{(g + \tilde{p}u)}{\tilde{p}^2} (\cos \tilde{p}t - 1)
\end{aligned}
\tag{7.6}
$$

where t denotes time. In expanded form we have

$$
\begin{aligned}
x &= ut - (g + \tilde{p}u)\tilde{p} \cdot \frac{t^2}{6} \ldots \\
y &= -(g + \tilde{p}u) \frac{t^2}{2} \ldots \quad .
\end{aligned}
\tag{7.7}
$$

This agrees with (7.5).

Appendix

I

$$\int_{-1}^{\infty} \frac{1}{\sigma} \ell n^2\left(\frac{\sqrt{\sigma+1}-1}{\sqrt{\sigma+1}+1}\right) d\sigma = \int_{-1}^{-\infty} \frac{1}{\sigma} \ell n^2\left(\frac{\sqrt{\sigma+1}-1}{\sqrt{\sigma+1}+1}\right) d\sigma$$

$$= \int_{-1}^{\infty} \frac{1}{\sigma} \ell n^2\left(\frac{i\sqrt{\sigma-1}-1}{i\sqrt{\sigma-1}+1}\right) d\sigma \qquad (\sigma = \csc^2 \tfrac{\theta}{2})$$

$$= -\int_{0}^{\pi} \theta^2 \cot \frac{\theta}{2}\, d\theta = 4 \int_{0}^{\pi} \theta \ \ell n\ (\sin \tfrac{\theta}{2}) d\theta$$

$$= -\pi^2 2 \ell n\ 2 - 4\left[\sum_{n=1}^{\infty} \frac{\cos n\pi}{n^3} - \sum_{n=1}^{\infty} \frac{1}{n^3}\right]$$

$$\left(\sum_{n=1}^{\infty} \frac{1}{n^3} = 1.2020569032\right)$$

$$\text{(A.1)} \qquad \int_{-1}^{\infty} \frac{1}{\sigma} \ell n^2\left(\frac{\sqrt{\sigma+1}-1}{\sqrt{\sigma+1}+1}\right) d\sigma = -\pi^2 2 \ell n\ 2 + 8.416$$

II

$$\int_{-1}^{-\infty} \frac{[\omega_1(\lambda) - \omega_1(\infty)]}{\lambda\sqrt{\lambda+1}}\, d\lambda = i\pi\omega_1(\infty) + \frac{i(\bar{p}+1)}{\pi^2} \int_{-1}^{-\infty} \frac{1}{\lambda} \ell n^2\left(\frac{\sqrt{\lambda+1}-1}{\sqrt{\lambda+1}+1}\right) d\lambda$$

$$\text{(A.2)} \qquad \int_{-1}^{-\infty} \frac{[\omega_1(\lambda) - \omega_1(\infty)]}{\lambda\sqrt{\lambda+1}}\, d\lambda = \frac{i(\bar{p}+1)(8.416)}{\pi^2}$$

III

$$\int_{-1}^{-\infty} \frac{[\omega_1(\lambda) - \omega_1(\infty)]}{\lambda}\, d\lambda = \frac{i(\bar{p}+1)}{\pi^2} \int_{1}^{\infty} \frac{\ell n\ \sigma}{\sigma}\ \ell n\left(\frac{i\sqrt{\sigma-1} - 1}{i\sqrt{\sigma-1} + 1}\right) d\sigma$$

$$(\sigma = \csc^2\theta)$$

$$= -\frac{4(\bar{p}+1)}{\pi^2} \int_{0}^{\pi/2} \ell n^2(\sin\theta) d\theta$$

$$= -\frac{(\bar{p}+1)}{\pi^2} \frac{d^2}{dx^2} \int_{0}^{\pi/2} (\sin\theta)^{2x}\, d\theta \Big|_{x=0}$$

$$= -\frac{(\bar{p}+1)}{\pi^2} \frac{d^2}{dx^2} \frac{\Gamma(x+\frac{1}{2})\Gamma(\frac{1}{2})}{2\Gamma(x+1)} \Big|_{x=0}$$

$$\text{(A.3)} \qquad \int_{-1}^{-\infty} \frac{[\omega_1(\lambda) - \omega_1(\infty)]}{\lambda}\, d\lambda = -\frac{(\bar{p}+1)}{2\pi} \left[(2\ \ell n\ 2)^2 + \frac{\pi^2}{3}\right]$$

IV

$$\int_{\zeta}^{\infty} \frac{1}{\sigma}\ \ell n^2\left(\frac{\sqrt{\sigma+1} - 1}{\sqrt{\sigma+1} + 1}\right) d\sigma = \int_{\frac{\sqrt{\zeta+1} - 1}{\sqrt{\zeta+1} + 1}}^{1} \left(\frac{1}{u} + \frac{2}{1-u}\right) \ell n^2 u\ du$$

$$\left(\frac{\sqrt{\sigma+1} - 1}{\sqrt{\sigma+1} + 1} = u\right)$$

$$= -\frac{1}{3}\ \ell n^3 \frac{\zeta}{(\sqrt{\zeta+1} + 1)^2} + 2 \int_{\frac{\sqrt{\zeta+1} - 1}{\sqrt{\zeta+1} + 1}}^{1} \frac{\ell n^2 u}{1-u}\ du$$

$$\lim_{\zeta \to 0} \int_{\zeta}^{\infty} \frac{1}{\sigma} \ln^2 \left(\frac{\sqrt{\sigma+1} - 1}{\sqrt{\sigma+1} + 1} \right) d\sigma = -\frac{1}{3} \lim_{\zeta \to 0} (\ln \zeta - 2 \ln 2)^3 + 2 \int_0^1 \frac{\ln^2 u}{1-u} du$$

$$= -\frac{1}{3} \lim_{\zeta \to 0} (\ln \zeta - 2 \ln 2)^3 + 4 \sum_{n=1}^{\infty} \frac{1}{n^3}$$

$$\text{(A.4)} \quad \lim_{\zeta \to 0} \int_{\zeta}^{\infty} \frac{1}{\sigma} \ln^2 \left(\frac{\sqrt{\sigma+1} - 1}{\sqrt{\sigma+1} + 1} \right) d\sigma = -\frac{1}{3} \lim_{\zeta \to 0} (\ln \zeta - 2 \ln 2)^3 + 4.808$$

V

$$\int_{\zeta}^{\infty} \frac{[\omega_1(\sigma) - \omega_1(\infty)]}{\sigma} d\sigma = -[\omega_1(\zeta) - \omega_1(\infty)] \ln \zeta$$

$$+ \frac{i(\bar{p}+1)}{\pi^2} \int_{\zeta}^{\infty} \frac{\ln \sigma}{\sigma} \ln \left(\frac{\sqrt{\sigma+1} - 1}{\sqrt{\sigma+1} + 1} \right) d\sigma$$

$$= -[\omega_1(\zeta) - \omega_1(\infty)] \ln \zeta - \frac{i(\bar{p}+1)}{2\pi^2} \ln^2 \zeta \ln \left(\frac{\sqrt{\zeta+1} - 1}{\sqrt{\zeta+1} + 1} \right)$$

$$- \frac{i(\bar{p}+1)}{2\pi^2} \int_{\zeta}^{\infty} \frac{\ln^2 \sigma}{\sigma \sqrt{\sigma+1}} d\sigma$$

$$= -[\omega_1(\zeta) - \omega_1(\infty)] \ln 2 - \frac{i(\bar{p}+1)}{2\pi^2} \ln^2 \zeta \ln \left(\frac{\sqrt{\zeta+1} - 1}{\sqrt{\zeta+1} + 1} \right)$$

$$+ \frac{i(\bar{p}+1) \ln^3 \zeta}{6\pi^2 \sqrt{\zeta+1}} - \frac{i(\bar{p}+1)}{12\pi^2} \int_{\zeta}^{\infty} \frac{\ln^3 \sigma}{(\sigma+1)^{3/2}} d\sigma$$

$$\lim_{\zeta\to 0}\int_{\zeta}^{\infty}\frac{[\omega_1(\sigma)-\omega_1(\infty)]}{\sigma}\,d\sigma = -\lim_{\zeta\to 0}[\omega_1(\zeta)-\omega_1(\infty)]\ell n\ \zeta$$

$$-\frac{i(\bar{p}+1)}{2\pi^2}\lim_{\zeta\to 0}\ell n^2\zeta(\ell n\ \zeta - 2\ \ell n\ 2)$$

$$+\frac{i(\bar{p}+1)}{6\pi^2}\lim_{\zeta\to 0}\ell n^3\zeta - \frac{i(\bar{p}+1)}{12\pi^2}\int_0^{\infty}\frac{\ell n^3\sigma}{(\sigma+1)^{3/2}}\,d\sigma$$

$$\int_0^{\infty}\frac{\ell n^3\sigma}{(\sigma+1)^{3/2}}\,d\sigma = \frac{d^3}{dx^3}\int_0^{\infty}\frac{\sigma^x}{(\sigma+1)^{3/2}}\,d\sigma\Bigg|_{x=0}$$

$$= \frac{d^3}{dx^3}\int_1^{\infty}\frac{(u-1)^x}{u^{3/2}}\,du\Bigg|_{x=0}$$

$$= \frac{d^3}{dx^3}\frac{\Gamma(\frac{1}{2}-x)\Gamma(1+x)}{\Gamma(\frac{3}{2})}\Bigg|_{x=0}$$

$$= 2\left\{(2\ \ell n\ 2)^3 + 4\pi^2\ \ell n\ 2 + 12\sum_{n=1}^{\infty}\frac{1}{n^3}\right\}$$

(A.5) $$\lim_{\zeta\to 0}\int_{\zeta}^{\infty}\frac{[\omega_1(\sigma)-\omega_1(\infty)]}{\sigma}\,d\sigma$$

$$= \frac{i(\bar{p}+1)}{6\pi^2}\lim_{\zeta\to 0}\left\{\begin{array}{l} 2\pi^2(\ell n\ \zeta - 2\ \ell n\ 2) \\ +\ (\ell n\ \zeta - 2\ \ell n\ 2)^3 \\ -\ 12\sum_{n=1}^{\infty}\frac{1}{n^3}\end{array}\right\}$$

$$\frac{1}{\pi^2}\int_{-1}^{-\infty}\frac{[\omega_1(\lambda)-\omega_1(\alpha)]}{\sqrt{\lambda+1}}\left[-\frac{2\sqrt{-\lambda-1}}{\lambda}\arctan\frac{1}{\sqrt{-\lambda-1}}\right]d\lambda$$

$$=\frac{2i}{\pi^2}\int_{1}^{\infty}\frac{1}{\lambda}\arctan\frac{1}{\sqrt{\lambda-1}}\int_{\infty}^{-\lambda}\omega_1'(\sigma)d\sigma d\lambda$$

$$=\frac{2(\bar{p}+1)}{\pi^4}\int_{1}^{\infty}\frac{1}{\lambda}\arctan\frac{1}{\sqrt{\lambda-1}}\int_{-\infty}^{\lambda}\frac{1}{u}\ln\left(\frac{i\sqrt{u-1}-1}{i\sqrt{u-1}+1}\right)dud\lambda$$

$$=\frac{4i(\bar{p}+1)}{\pi^4}\int_{1}^{\infty}\frac{1}{\lambda}\arctan\frac{1}{\sqrt{\lambda-1}}\int_{\infty}^{\lambda}\frac{1}{u}\arctan\frac{1}{\sqrt{u-1}}dud\lambda$$

$$=-\frac{2i(\bar{p}+1)}{\pi^4}\left[\int_{1}^{\infty}\frac{1}{u}\arctan\frac{1}{\sqrt{u-1}}du\right]^2$$

$$\int_{1}^{\infty}\frac{1}{u}\arctan\frac{1}{\sqrt{u-1}}du=\frac{1}{2}\int_{1}^{\infty}\frac{\ln u}{u\sqrt{u-1}}du$$

$$=-\frac{1}{2}\int_{0}^{1}\frac{\ln v\,dv}{v^{1/2}(1-v)^{1/2}}$$

$$=-\frac{1}{2}\frac{d}{dx}\int_{0}^{1}v^{x-1}(1-v)^{\frac{1}{2}-1}dv\Bigg|_{x=1/2}$$

$$=-\frac{1}{2}\frac{d}{dx}\frac{\Gamma(x)\Gamma(\frac{1}{2})}{\Gamma(x+\frac{1}{2})}\Bigg|_{x=1/2}$$

$$=\pi\ln 2$$

(A.6) $$\frac{1}{\pi^2}\int_{-1}^{-\infty}\frac{[\omega_1(\lambda)-\omega_1(\infty)]}{\sqrt{\lambda+1}}\left[-\frac{2\sqrt{-\lambda-1}}{\lambda}\arctan\frac{1}{\sqrt{-\lambda-1}}\right]d\lambda$$

$$= -\frac{i(\bar{p}+1)(2\ \ell n\ 2)^2}{2\pi^2}$$

VII

$$\frac{2}{\pi^2}\int_{-1}^{-\infty}\frac{[\omega_1(\lambda)-\omega_1(\infty)]}{\lambda}\arctan\frac{\sqrt{\xi+1}}{\sqrt{-\lambda-1}}\,d\lambda$$

$$= -\frac{2(\bar{p}+1)}{\pi^4}\int_1^{\infty}\left(\frac{4}{\sqrt{\pi}}\sum_{k=0}^{\infty}\frac{\Gamma(\frac{1}{2}+k)}{k!(2k+1)2\lambda^{k+\frac{3}{2}}}\right)\cdot\arctan\frac{\sqrt{\xi+1}}{\sqrt{\lambda-1}}\,d\lambda$$

$$= -\frac{(\bar{p}+1)}{\pi^2}\left[2\ \ell n^2\,2+\frac{\pi^2}{6}\right]$$

$$+\frac{(\bar{p}+1)}{\pi^4}\int_1^{\infty}\frac{\sqrt{\xi+1}}{\sqrt{\lambda-1}\ (\lambda+\xi)}\int_{\lambda}^{\infty}\frac{4}{\sqrt{\pi}}\sum_{k=0}^{\infty}\frac{\Gamma(\frac{1}{2}+k)}{k!(2k+1)2\sigma^{k+\frac{3}{2}}}\,d\sigma d\lambda$$

$$(\bar{p}+1) > 0$$

$$\frac{2}{\pi^2}\int_1^{\infty}\frac{[\omega_1(-\lambda)-\omega_1(\infty)]}{\lambda}\arctan\frac{\sqrt{\xi+1}}{\sqrt{\lambda-1}}\,d\lambda$$

$$< -\frac{8(\bar{p}+1)}{\pi^4}\int_1^{\infty}\frac{1}{\lambda^{3/2}}\arctan\frac{\sqrt{\xi+1}}{\sqrt{\lambda-1}}\,d\lambda$$

$$< -\frac{8(\bar{p}+1)}{\pi^4}\left[\pi-\frac{2}{\sqrt{\xi}}\ell n\left(\sqrt{1+\xi}+\sqrt{\xi}\right)\right]$$

$$\frac{2}{\pi^2}\int_1^{\infty}\frac{[\omega_1(-\lambda)-\omega_1(\infty)]}{\lambda}\arctan\frac{\sqrt{\xi+1}}{\sqrt{\lambda-1}}\,d\lambda$$

$$> -\frac{(\bar{p}+1)}{\pi^2}\left[2\ln^2 2+\frac{\pi^2}{6}\right]+\frac{4(\bar{p}+1)}{\pi^4}\int_1^{\infty}\frac{\sqrt{\xi+1}}{\sqrt{\lambda-1}\,(\lambda+\xi)}\int_{\lambda}^{\infty}\frac{d\sigma}{\sigma^{3/2}}\,d\lambda$$

$$> -\frac{(\bar{p}+1)}{\pi^2}\left[2\ln^2 2+\frac{\pi^2}{6}\right]+\frac{16(\bar{p}+1)}{\pi^4}\cdot\frac{1}{\sqrt{\xi}}\ln\left(\sqrt{1+\xi}+\sqrt{\xi}\right)$$

$$(\bar{p}+1) > 0$$

(A.7)
$$\frac{16(\bar{p}+1)}{\pi^4}\cdot\frac{1}{\sqrt{\xi}}\ln\left(\sqrt{1+\xi}+\sqrt{\xi}\right)-\frac{(\bar{p}+1)}{\pi^2}\left[2\ln^2 2+\frac{\pi^2}{6}\right]$$

$$< \frac{2}{\pi^2}\int_1^{\infty}\frac{[\omega_1(-\lambda)-\omega_1(\infty)]}{\lambda}\arctan\frac{\sqrt{\xi+1}}{\sqrt{\lambda-1}}\,d\lambda$$

$$< -\frac{8(\bar{p}+1)}{\pi^3}+\frac{16(\bar{p}+1)}{\pi^4}\cdot\frac{1}{\sqrt{\xi}}\ln\left(\sqrt{1+\xi}+\sqrt{\xi}\right)$$

$$\frac{1}{\pi^2}\left(2\ln^2 2+\frac{\pi^2}{6}-\frac{8}{\pi}\right)=.00597$$

References

[1] Rouse, H., Discharge Characteristics of the Free Overfall, Civil Engineering, Vol. 6, April 1936, p. 257.

[2] Southwell, R. V. and Vaisey, G., Relaxation Methods Applied to Engineering Problems: XII, Fluid Motions Characterized by Free Streamlines, Phil. Trans. Roy. Soc. (London), A, Vol. 240 (1946), p. 117.

[3] Jaeger, C., Hauteur d'eau a l'extremité d'un long déversoir, La Houille Blanche, Vol. 3, part 6 (1948), p. 518.

[4] Roy, S. K., Note on the Stream Depth at the Edge of a Free Overfall, La Houille Blanche, Vol. 4, part 6 (1949). p. 832.

[5] Fraser, W. B., Gravity-deflected Jets in Two-Dimensional Flow, M.E. Thesis, University of Canterbury, N.Z. (May 1961).

[6] Hay, H. and Markland, E., The Determination of the Discharge over Weirs by the Electrolytic Tank, Proc. I.C.E. (London) Vol. 10, May 1958, p. 59.

Security Classification

DOCUMENT CONTROL DATA - R&D

(Security classification of title, body of abstract and indexing annotation must be entered when the overall report is classified)

1. ORIGINATING ACTIVITY (Corporate author)	2a. REPORT SECURITY CLASSIFICATION
Courant Institute of Mathematical Sciences New York University	not classified
	2b GROUP none

3. REPORT TITLE

Supercritical Flow in an Overfall

4. DESCRIPTIVE NOTES *(Type of report and inclusive dates)*

Technical Report-September 1970

5. AUTHOR(S) *(Last name, first name, initial)*

Peters, Arthur S.

6. REPORT DATE	7a. TOTAL NO. OF PAGES	7b. NO. OF REFS
September 1970	47	6

8a. CONTRACT OR GRANT NO.	9a. ORIGINATOR'S REPORT NUMBER(S)
N00014-67-A-0467-0016 b. PROJECT NO. NR 062-160	IMM 384
c. d.	9b. OTHER REPORT NO(S) *(Any other numbers that may be assigned this report)* none

10. AVAILABILITY/LIMITATION NOTICES

Distribution of this document is unlimited.

11. SUPPLEMENTARY NOTES	12. SPONSORING MILITARY ACTIVITY
none	U.S. Navy, Office of Naval Research 207 West 24th St., New York, N.Y.

13. ABSTRACT

This report presents an analysis of supercritical flow in an overfall whose nappes are subjected to different constant pressures. It contains computations for brink depth and approximate equations for the nappes in the neighborhood of the brink and far downstream.

DD FORM 1 JAN 64 1473

Security Classification

14 KEY WORDS	LINK A		LINK B		LINK C	
	ROLE	WT	ROLE	WT	ROLE	WT

INSTRUCTIONS

1. ORIGINATING ACTIVITY: Enter the name and address of the contractor, subcontractor, grantee, Department of Defense activity or other organization *(corporate author)* issuing the report.

2a. REPORT SECURITY CLASSIFICATION: Enter the overall security classification of the report. Indicate whether "Restricted Data" is included. Marking is to be in accordance with appropriate security regulations.

2b. GROUP: Automatic downgrading is specified in DoD Directive 5200.10 and Armed Forces Industrial Manual. Enter the group number. Also, when applicable, show that optional markings have been used for Group 3 and Group 4 as authorized.

3. REPORT TITLE: Enter the complete report title in all capital letters. Titles in all cases should be unclassified. If a meaningful title cannot be selected without classification, show title classification in all capitals in parenthesis immediately following the title.

4. DESCRIPTIVE NOTES: If appropriate, enter the type of report, e.g., interim, progress, summary, annual, or final. Give the inclusive dates when a specific reporting period is covered.

5. AUTHOR(S): Enter the name(s) of author(s) as shown on or in the report. Enter last name, first name, middle initial. If military, show rank and branch of service. The name of the principal author is an absolute minimum requirement.

6. REPORT DATE: Enter the date of the report as day, month, year, or month, year. If more than one date appears on the report, use date of publication.

7a. TOTAL NUMBER OF PAGES: The total page count should follow normal pagination procedures, i.e., enter the number of pages containing information.

7b. NUMBER OF REFERENCES: Enter the total number of references cited in the report.

8a. CONTRACT OR GRANT NUMBER: If appropriate, enter the applicable number of the contract or grant under which the report was written.

8b, 8c, & 8d. PROJECT NUMBER: Enter the appropriate military department identification, such as project number, subproject number, system numbers, task number, etc.

9a. ORIGINATOR'S REPORT NUMBER(S): Enter the official report number by which the document will be identified and controlled by the originating activity. This number must be unique to this report.

9b. OTHER REPORT NUMBER(S): If the report has been assigned any other report numbers *(either by the originator or by the sponsor)*, also enter this number(s).

10. AVAILABILITY/LIMITATION NOTICES: Enter any limitations on further dissemination of the report, other than those imposed by security classification, using standard statements such as:

(1) "Qualified requesters may obtain copies of this report from DDC."

(2) "Foreign announcement and dissemination of this report by DDC is not authorized."

(3) "U. S. Government agencies may obtain copies of this report directly from DDC. Other qualified DDC users shall request through

_____."

(4) "U. S. military agencies may obtain copies of this report directly from DDC. Other qualified users shall request through

_____."

(5) "All distribution of this report is controlled. Qualified DDC users shall request through

_____."

If the report has been furnished to the Office of Technical Services, Department of Commerce, for sale to the public, indicate this fact and enter the price, if known.

11. SUPPLEMENTARY NOTES: Use for additional explanatory notes.

12. SPONSORING MILITARY ACTIVITY: Enter the name of the departmental project office or laboratory sponsoring *(paying for)* the research and development. Include address.

13. ABSTRACT: Enter an abstract giving a brief and factual summary of the document indicative of the report, even though it may also appear elsewhere in the body of the technical report. If additional space is required, a continuation sheet shall be attached.

It is highly desirable that the abstract of classified reports be unclassified. Each paragraph of the abstract shall end with an indication of the military security classification of the information in the paragraph, represented as *(TS), (S), (C), or (U)*

There is no limitation on the length of the abstract. However, the suggested length is from 150 to 225 words.

14. KEY WORDS: Key words are technically meaningful terms or short phrases that characterize a report and may be used as index entries for cataloging the report. Key words must be selected so that no security classification is required. Identifiers, such as equipment model designation, trade name, military project code name, geographic location, may be used as key words but will be followed by an indication of technical context. The assignment of links, roles, and weights is optional.

Technical Library
Building 131
Aberdeen Proving Ground, Maryland 21005

Defense Documentation Center (20)
Cameron Station
Alexandria, Virginia 22314

Technical Library
Naval Ship Research and
Development Center
Annapolis Division
Annapolis, Maryland 21402

Professor Bruce Johnson
Engineering Department
Naval Academy
Annapolis, Maryland 21402

Library
Naval Academy
Annapolis, Maryland 21402

Professor W. P. Graebel
Department of Engineering
Mechanics
The University of Michigan
College of Engineering
Ann Arbor, Michigan 48104

Professor W. R. Debler
Department of Engineering Mechanics
University of Mechanics
Ann Arbor, Michigan 48108

Dr. Francis Ogilvie
Department of Naval Architecture
and Marine Engineering
University of Michigan
Ann Arbor, Michigan 48108

Professor S. D. Sharma
Department of Naval Architecture
and Marine Engineering
University of Michigan
Ann Arbor, Michigan 48108

Professor W. W. Willmarth
Department of Aerospace Engineering
University of Michigan
Ann Arbor, Michigan 48108

Professor Finn C. Michelsen
Naval Architecture and Marine
Engineering
445 West Engineering Bldg.
University of Michigan
Ann Arbor, Michigan 48104

AFOSR (REM)
1400 Wilson Boulevard
Arlington, Virginia 22204

Dr. J. Menkes
Institute for Defense Analyses
400 Army-Navy Drive
Arlington, Virginia 22204

Professor S. Corrsin
Mechanics Department
The Johns Hopkins University
Baltimore, Maryland 20910

Professor L. S. G. Kovasznay
The Johns Hopkins University
Baltimore, Maryland 20910

Librarian
Department of Naval Architecture
University of California
Berkeley, California 94720

Professor P. Lieber
Department of Mechanical Engineering
University of California
Institute of Engineering Research
Berkeley, California 94720

Professor M. Holt
Division of Aeronautical Sciences
University of California
Berkeley, California 94720

Professor J. V. Wehausen
Department of Naval Architecture
University of California
Berkeley, California 94720

Professor J. R. Paulling
Department of Naval Architecture
University of California
Berkeley, California 94720

Professor E. V. Laitone
Department of Mechanical Engineering
University of California
Berkeley, California 94720

School of Applied Mathematics
Indiana University
Bloomington, Indiana 47401

Commander
Boston Naval Shipyard
Boston, Massachusetts 02129

Director
Office of Naval Research
Branch Office
495 Summer Street
Boston, Massachusetts 02210

Professor M. S. Uberoi
Department of Aeronautical Engineering
University of Colorado
Boulder, Colorado 80303

Naval Applied Science Laboratory
Technical Library
Bldg. 1 Code 222
Flushing and Washington Avenues
Brooklyn, New York 11251

Professor J. J. Foody
Chairman, Engineering Department
State University of New York
Maritime College
Bronx, New York 10465

Dr. Irving C. Statler, Head
Applied Mechanics Department
Cornell Aeronautical Laboratory, Inc.
P. O. Box 235
Buffalo, New York 14221

Dr. Alfred Ritter
Assistant Head, Applied Mechanics Dept.
Cornell Aeronautical Laboratory, Inc.
Buffalo, New York 14221

Professor G. Birkhoff
Department of Mathematics
Harvard University
Cambridge, Massachusetts 02138

Commanding Officer
NROTC Naval Administrative Unit
Massachusetts Institute of Technology
Cambridge, Massachusetts 02139

Professor N. Newman
Department of Naval Architecture and
Marine Engineering
Massachusetts Institute of Technology
Cambridge, Massachusetts 02139

Professor A. H. Shapiro
Department of Mechanical Engineering
Massachusetts Institute of Technology
Cambridge, Massachusetts 02139

Professor C. C. Lin
Department of Mathematics
Massachusetts Institute of Technology
Cambridge, Massachusetts 02139

Professor E. W. Merrill
Department of Mathematics
Massachusetts Institute of Technology
Cambridge, Massachusetts 02139

Professor M. A. Abkowitz
Department of Naval Architecture
and Marine Engineering
Massachusetts Institute of Technology
Cambridge, Massachusetts 02139

Professor G. H. Carrier
Department of Engineering and
Applied Physics
Harvard University
Cambridge, Massachusetts 02139

Professor E. Mollo-Christensen
Room 54-1722
Massachusetts Institute of Technology
Cambridge, Massachusetts 02139

Professor A. T. Ippen
Department of Civil Engineering
Massachusetts Institute of Technology
Cambridge, Massachusetts 02139

Commander
Charleston Naval Shipyard
U. S. Naval Base
Charleston, South Carolina 29408

A. R. Kuhlthau, Director
Research Laboratories for the
Engineering Sciences
Thorton Hall, University of Virginia
Charlottesville, Virginia 22903

Director
Office of Naval Research
Branch Office
219 Dearborn Street
Chicago, Illinois 60604

Library
Naval Weapons Center
China Lake, California 93557

Library MS 60-3
NASA Lewis Research Center
21000 Brookpark Road
Cleveland, Ohio 44135

Professor J. M. Burgers
Institute of Fluid Dynamics and
Applied Mathematics
University of Maryland
College Park, Maryland 20742

Acquisition Director
NASA Scientific & Technical
Information
P. O. Box 33
College Park, Maryland 20740

Professor Pai
Institute for Fluid Dynamics
and Applied Mathematics
University of Maryland
College Park, Maryland 20740

Technical Library
Naval Weapons Laboratory
Dahlgren, Virginia 22448

Computation & Analyses Laboratory
Naval Weapons Laboratory
Dahlgren, Virginia 22448

Professor C. S. Wells
LTV Research Center
Dallas, Texas 75222

Dr. R. H. Kraichnan
Dublin, New Hampshire 03444

Commanding Officer
Army Research Office
Box CM, Duke Station
Durham, North Carolina 27706

Professor A. Charnes
The Technological Institute
Northwestern University
Evanston, Illinois 60201

Dr. Martim H. Bloom
Polytechnic Institute of Brooklyn
Graduate Center, Dept. of Aerospace
Engineering and Applied Mechanics
Farmingdale, New York 11735

Technical Documents Center
Building 315
U. S. Army Mobility Equipment
Research and Development Center
Fort Belvoir, Virginia 22060

Professor J. E. Cermak
College of Engineering
Colorado State University
Ft. Collins, Colorado 80521

Technical Library
Webb Institute of Naval Architecture
Glen Cove, Long Island, New York 11542

Professor E. V. Lewis
Webb Institute of Naval Architecture
Glen Cove, Long Island, New York 11542

Library MS 185
NASA, Langley Research Center
Langley Station
Hampton, Virginia 23365

Dr. B. N. Pridmore Brown
Northrop Corporation
NORAIR-Div.
Hawthorne, California 90250

Dr. J. P. Breslin
Stevens Institute of Technology
Davidson Laboratory
Hoboken, New Jersey 07030

Mr. D. Savitsky
Stevens Institute of Technology
Davidson Laboratory
Hoboken, New Jersey 07030

Mr. C. H. Henry
Stevens Institute of Technology
Davidson Laboratory
Hoboken, New Jersey 07030

Professor J. F. Kennedy, Director
Iowa Institute of Hydraulic Research
State University of Iowa
Iowa City, Iowa 52240

Professor L. Landweber
Iowa Institute of Hydraulic Research
State University of Iowa
Iowa City, Iowa 52240

Professor E. L. Resler
Graduate School of
Aeronautical Engineering
Cornell University
Ithaca, New York 14851

Professor John Miles
% I.G.P.P.
University of California, San Diego
La Jolla, California 92038

Director
Scripps Institution of Oceanography
University of California
La Jolla, California 92037

Dr. B. Sternlicht
Mechanical Technology Incorporated
968 Albany-Shaker Road
Latham, New York 12110

Mr. P. Eisenberg, President
Hydronautics
Pindell School Road
Howard County
Laurel, Maryland 20810

(2)

Professor A. Ellis
University of California, San Diego
Department of Aerospace & Mech. Engrg. Sci.
La Jolla, California 92037

Mr. Alfonso Alvarado L. Director
Laboratorio Nacional De Hydraulics
Antigui Carretera A. Ancon
Casilla Postal 682
Lima, Peru

Commander
Long Beach Naval Shipyard
Long Beach, California 90802

Professor John Laufer
Department of Aerospace Engineering
University Park
Los Angeles, California 90007

Professor J. Ripkin
St. Anthony Falls Hydraulic Lab.
University of Minnesota
Minneapolis, Minnesota 55414

Professor J. M. Killen
St. Anthony Falls Hydraulic Lab.
University of Minnesota
Minneapolis, Minnesota 55414

Lorenz G. Straub Library
St. Anthony Falls Hydraulic Lab.
Mississippi River at 3rd Avenue SE.
Minneapolis, Minnesota 55414

Dr. E. Silberman
St. Anthony Falls Hydraulic Lab.
University of Minnesota
Minneapolis, Minnesota 55414

Superintendent
Naval Postgraduate School
Library Code 0212
Monterey, California 93940

Professor A. B. Metzner
University of Delaware
Newark, New Jersey 19711

Technical Library
USN Underwater Weapons &
Research & Engineering Station
Newport, Rhode Island 02840

Technical Library
Underwater Sound Laboratory
Fort Trumbull
New London, Connecticut 06320

Professor J. J. Stoker
Institute of Mathematical Sciences
New York University
251 Mercer Street
New York, New York 10003

Engineering Societies Library
345 East 47th Street
New York, New York 10017

Office of Naval Research
New York Area Office
207 W. 24th Street
New York, New York 10011

Professor H. Elrod
Department of Mechanical Engineering
Columbia University
New York, New York 10027

Society of Naval Architects and
Marine Engineering
74 Trinity Place
New York, New York 10006

Professor S. A. Piascek
Department of Engineering Mechanics
University of Notre Dame
Notre Dame, Indiana 46556

United States Atomic Energy Commission
Division of Technical Information
Extension
P. O. Box 62
Oak Ridge, Tennessee 37830

Miss O. M. Leach, Librarian
National Research Council
Aeronautical Library
Montreal Road
Ottawa 7, Canada

Technical Library
Naval Ship Research and
Development Center
Panaman City, Florida 32401

Library
Jet Propulsion Laboratory
California Institute of Technology
4800 Oak Grove Avenue
Pasadena, California 91109

Professor M. S. Plesset
Engineering Division
California Institute of Technology
Pasadena, California 91109

Professor H. Liepmann
Department of Aeronautics
California Institute of Technology
Pasadena, California 91109

Technical Library
Naval Undersea Warfare Center
3202 E. Foothill Boulevard
Pasadena, California 91107

Dr. J. W. Hoyt
Naval Undersea Warfare Center
3202 E. Foothill Boulevard
Pasadena, California 91107

Professor T. Y. Wu
Department of Engineering
California Institute of Technology
Pasadena, California 91109

Director
Office of Naval Research
Branch Office
1030 E. Green Street
Pasadena, California 91101

Professor A. Acosta
Department of Mechanical Engineering
California Institute of Technology
Pasadena, California 91109

Naval Ship Engineering Center
Philadelphia Division
Technical Library
Philadelphia, Pennsylvania 19112

Technical Library (Code 249B)
Philadelphia Naval Shipyard
Philadelphia, Pennsylvania 19112

Professor R. C. Mac Camy
Department of Mathematics
Carnegie Institute of Technology
Pittsburgh, Pennsylvania 15213

Dr. Paul Kaplan
Oceanics, Inc.
Plainview, Long Island, New York 11803

Technical Library
Naval Missile Center
Point Mugu, California 93041

Technical Library
Naval Civil Engineering Lab.
Port Hueneme, California 93041

Commander
Portsmouth Naval Shipyard
Portsmouth, New Hampshire 03801

Commander
Norfolk Naval Shipyard
Portsmouth, Virginia 23709

Professor F. E. Bisshopp
Division of Engineering
Brown University
Providence, Rhode Island 02912

Dr. L. L. Higgins
TRW Space Technology Labs, Inc.
One Space Park
Redondo Beach, California 90278

Redstone Scientific Information Center
Attn: Chief, Document Section
Army Missile Command
Redstone Arsenal, Alabama 35809

Dr. H. N. Abramson
Southwest Research Institute
8500 Culebra Road
San Antonio, Texas 78228

Editor
Applied Mechanics Review
Southwest Research Institute
8500 Culebra Road
San Antonio, Texas 78206

Librarian
Naval Command Control Communications
Laboratory Center
San Diego, California 92152

Library & Information Services
General Dynamics-Convair
P. O. Box 1128
San Diego, California 92112

Commander (Code 246P)
Pearl Harbor Naval Shipyard
Box 400
FPO San Francisco, California 96610

Technical Library (Code H245C-3)
Hunters Point Division
San Francisco Bay Naval Shipyard
San Francisco, California 94135

Dr. A. May
Naval Ordnance Laboratory
White Oak
Silver Spring, Maryland 20910

Fenton Kennedy Document Library
The Johns Hopkins University
Applied Physics Laboratory
8621 Georgia Avenue
Silver Spring, Maryland 20910

Librarian
Naval Ordnance Laboratory
White Oak
Silver Spring, Maryland 20910

Dr. Bryne Perry
Department of Civil Engineering
Stanford University
Stanford, California 94305

Professor Milton Van Dyke
Department of Aeronautical Engineering
Stanford University
Stanford , California 94305

Professor E. Y. Hsu
Department of Civil Engineering
Stanford University
Stanford, California 94305

Dr. R. L. Street
Department of Civil Engineering
Stanford University
Stanford, California 94305

Professor S. Eskinazi
Department of Mechanical Engineering
Syracuse University
Syracuse, New York 13210

Professor R. Pfeffer
Florida State University
Geophysical Fluid Dynamics Institute
Tallahassee, Florida 32306

Professor J. Foa
Department of Aeronautical Engineering
Rennsselaer Polytechnic Institute
Troy, New York 12180

Professor R. C. Di Prima
Department of Mathematics
Rennsselaer Polytechnic Institute
Troy, New York 12180

Dr. M. Sevik
Ordnance Research Laboratory
Pennsylvania State University
University Park, Pennsylvania 16801

Professor J. Lumley
Ordnance Research Laboratory
Pennsylvania State University
University Park, Pennsylvania 16801

Dr. J. M. Robertson
Department of Theoretical and
Applied Mechanics
University of Illinois
Urbana, Illinois 61803

Shipyard Technical Library
Code 130L7 Building 746
San Francisco Bay Naval Shipyard
Vallejo, California 94592

Code L42
Naval Ship Research and
Development Center
Washington, D.C. 20007

Code 800
Naval Ship Research and
Development Center
Washington, D.C. 20007

Code 2027
U. S. Naval Research Laboratory
Washington, D.C. 20390 (6)

Code 438
Chief of Naval Research
Department of the Navy
Washington, D.C. 20360 (3)

Code 513
Naval Ship Research and
Development Center
Washington, D.C. 20007

Science & Technology Division
Library of Congress
Washington, D.C. 20540

ORD 913 (Library)
Naval Ordnance Systems Command
Washington, D.C. 20360

Code 6420
Naval Ship Engineering Center
Concept Design Division
Washington, D.C. 20360

Code 500
Naval Ship Research and
Development Center
Washington, D.C. 20007

Code 901
Naval Ship Research and
Development Center
Washington, D.C. 20007

Code 520
Naval Ship Research and
Development Center
Washington, D.C. 20007

Code 0341
Naval Ship Systems Command
Department of the Navy
Washington, D.C. 20360

Code 2052 (Technical Library)
Naval Ship Systems Command
Department of the Navy
Washington, D.C. 20360

Mr. J. L. Schuler (Code 03412)
Naval Ship Systems Command
Department of the Navy
Washington, D.C. 20360

Dr. J. H. Huth (Code 031)
Naval Ship Systems Command
Department of the Navy
Washington, D.C. 20360

Code 461
Chief of Naval Research
Department of the Navy
Washington, DC. 20360

Code 530
Naval Ship Research and
Development Center
Washington, D.C. 20360

Code 466
Chief of Naval Research
Department of the Navy
Washington, D.C. 20360

Office of Research and Development
Maritime Administration
441 G. Street, NW.
Washington, D.C. 20235

Code 463
Chief of Naval Research
Department of the Navy
Washington, D.C. 20360

National Science Foundation
Engineering Division
1800 G. Street, NW.
Washington, D.C. 20550

Dr. G. Kulin
National Bureau of Standards
Washington, D.C. 20234

Department of the Army
Coastal Engineering Research Center
5201 Little Falls Road, NW.
Washington, D.C. 20011

Code 521
Naval Ship Research and
Development Center
Washington, D.C. 20007

Code 481
Chief of Naval Research
Department of the Navy
Washington, D.C. 20390

Code 421
Chief of Naval Research
Department of the Navy
Washington, D.C. 20360

Commander
Naval Ordnance Systems Command
Code ORD 035
Washington, D.C. 20360

Librarian Station 5-2
Coast Guard Headquarters
1300 E. Street, NW.
Washington, D.C. 20226

Division of Ship Design
Maritime Administration
441 G. Street, NW.
Washington, D.C. 20235

HQ USAF (AFRSTD)
Room 1D 377
The Pentagon
Washington, D.C. 20330

Commander
Naval Ship Systems Command
Code 6644C
Washington, D.C. 20360

Code 525
Naval Ship Research and
Development Center
Washington, D.C. 20007

Dr. A. Powell (Code 01)
Naval Ship Research and
Development Center
Washington, D.C. 20007

Director of Research Code RR
National Aeronautics & Space Admin.
600 Independence Avenue, SW.
Washington, D.C. 20546

Commander
Naval Ordnance Systems Command
Code 03
Washington, D.C. 20360

Code ORD 05411
Naval Ordnance Systems Command
Washington, D.C. 20360

AIR 5301
Naval Air Systems Command
Department of the Navy
Washington, D.C. 20360

AIR 604
Naval Air Systems Command
Department of the Navy
Washington, D.C. 20360

Dr. John Craven (PM1100)
Deep Submergence Systems
Project
Department of the Navy
Washington, D.C. 20360

Code 522
Naval Ship Research and
Development Center
Washington, D.C. 20007

Commander
Naval Oceanographic Office
Washington, D.C. 20390

Chief of Research and Development
Office of Chief of Staff
Department of the Army
The Pentagon
Washington, D.C. 20310

Code 6342A
Naval Ship Systems Command
Department of the Navy
Washington, D.C.

Code 468
Chief of Naval Research
Department of the Navy
Washington, D.C. 20360

Director
U.S. Naval Research Laboratory
Code 6170
Washington, D.C. 20390

Code 473
Chief of Naval Research
Department of the Navy
Washington, D.C. 20360

Code 6100
Naval Ship Engineering Center
Department of the Navy
Washington, D.C. 20360

Mr. Ralph Lacey (Code 6114)
Naval Ship Engineering Center
Department of the Navy
Washington, D.C. 20360

Dr. A. S. Iberall, President
General Technical Services, Inc.
451 Penn Street
Yeadon, Pennsylvania 19050

Dr. H. Cohen
IBM Research Center
P. O. Box 218
Yorktown Heights, New York 10598

Director (25)
Naval Research Lab.
Code 2029 (ONR2)
Washington, D.C. 20390
Attn: Library

Stanford University
Department of Mathematics
Stanford, California

Office of Naval Research (2)
Department of the Navy (Code 432)
Washington, D.C. 20360

Office of Naval Research
San Francisco Area
50 Fell Street
San Francisco, California 94102

Library (2)
Courant Institute of Mathematical
Sciences
New York University
New York, New York 10012

Science Library
New York University
Brown 120
New York, New York 10012

Prof. O. M. Phillips
The Johns Hopkins University
Baltimore, Md. 20910

NOV 30 1970
DATE DUE

GAYLORD PRINTED IN U.S.A.